nature ecology & evolution

ARTICLES

https://doi.org/10.1038/s41559-019-1015-y

Promotion of protocell self-assembly from mixed amphiphiles at the origin of life

Sean F. Jordan[1], Hanadi Rammu[1], Ivan N. Zheludev[1], Andrew M. Hartley[2], Amandine Maréchal[2,3] and Nick Lane[1*]

Vesicles formed from single-chain amphiphiles (SCAs) such as fatty acids probably played an important role in the origin of life. A major criticism of the hypothesis that life arose in an early ocean hydrothermal environment is that hot temperatures, large pH gradients, high salinity and abundant divalent cations should preclude vesicle formation. However, these arguments are based on model vesicles using 1–3 SCAs, even though Fischer–Tropsch-type synthesis under hydrothermal conditions produces a wide array of fatty acids and 1-alkanols, including abundant C_{10}–C_{15} compounds. Here, we show that mixtures of these C_{10}–C_{15} SCAs form vesicles in aqueous solutions between pH ~6.5 and >12 at modern seawater concentrations of NaCl, Mg^{2+} and Ca^{2+}. Adding C_{10} isoprenoids improves vesicle stability even further. Vesicles form most readily at temperatures of ~70 °C and require salinity and strongly alkaline conditions to self-assemble. Thus, alkaline hydrothermal conditions not only permit protocell formation at the origin of life but actively favour it.

Membranes are fundamental to life, the nexus between cell and environment. Peter Mitchell wrote "I cannot consider the organism without its environment... From a formal point of view the two may be regarded as equivalent phases between which dynamic contact is maintained by the membranes that separate and link them"[1]. Beyond the requirement for compartmentalization, differences in ion concentration across the plasma membrane drive CO_2 fixation and energy metabolism in all modern autotrophic cells by vectorial chemistry[2–4]. This deep conservation of membrane bioenergetics also points to the fundamental role of membranes at the origin of life[2–4].

Despite their clear importance across life, the composition of early membranes is uncertain. The universality of membrane proteins with equivalent transmembrane helices indicates that early cells had some sort of lipid bilayer[5]. However, the phospholipid membranes of bacteria and archaea differ in their chemistry, most strikingly in the stereochemistry of their glycerol phosphate head groups—archaea typically have glycerol-1-phosphate while bacteria have glycerol-3-phosphate[6–8]. There is no known selective basis for this distinction[9], suggesting that their common ancestor did not possess a modern phospholipid membrane but instead had a simpler bilayer composed largely of single-chain amphiphiles (SCAs), perhaps including fatty acids and isoprenoids (which are found in both bacteria and archaea[10], and are perfectly compatible membrane components[11,12]). SCAs can assemble to form droplets, micelles or lipid bilayers in aqueous solutions depending on pH (Extended Data Fig. 1). Bilayer membranes composed of SCAs facilitate simple growth, being able to incorporate new lipids directly[13–15]. In principle, proton-permeable SCA membranes are also required for cells to harness geological ion gradients without collapsing to equilibrium, potentially shedding light on the deep divergence between bacteria and archaea[4,16].

The idea that the first cell membranes were composed of SCAs is appealing from the standpoint of prebiotic chemistry[17,18]. Fatty acid synthesis is thermodynamically favoured under mild hydrothermal conditions (25–150 °C) at alkaline pH (ref. [19]). Lipids have been synthesized from formate via Fischer–Tropsch-type reactions under hydrothermal conditions (100–150 °C), albeit in steel reactors, suggesting that iron (or carbon–metal bonds[20]) might be a critical electron donor or catalyst[21]. The lipids formed include abundant long-chain fatty acids and 1-alkanols (mainly C_6–C_{16})[21]. Likewise, the reaction of acetylene (C_2H_2) and CO in contact with nickel sulfide in hot aqueous medium at pH 7–9 can form unsaturated monocarboxylic acids (up to C_9)[22]. Branched-chain pentoses containing the isoprene skeleton are formed under mild alkaline hydrothermal conditions (60–90 °C, pH 9–11) via the formose reaction[23]. Higher pressure in submarine hydrothermal vents should favour synthesis of longer-chain amphiphiles, according to Le Chatelier's principle[21], as well as greatly increasing hydrogen solubility[24]. Thermophoresis in porous hydrothermal systems can concentrate amphiphiles above the critical bilayer concentration (CBC) to form vesicles spontaneously[25,26]. Mineral surfaces including silicates and FeS minerals found in hydrothermal systems can also enhance vesicle assembly[27]. Theoretical modelling suggests that vectorial CO_2 reduction on FeS clusters associated with protocell membranes (which are homologous to the proton-motive energy-converting hydrogenase in methanogens[28]) could drive protocellular growth and establish a rudimentary form of membrane heredity[29]. All of these factors point to alkaline hydrothermal systems as prebiotic electrochemical reactors[4,7,30–35] capable of driving the synthesis of amphiphiles, and then concentrating them in situ, to form protocells at the origin of life.

However, there is also a potentially serious drawback. One of the major criticisms of alkaline hydrothermal vents as a setting for the origin of life is that the relatively harsh environment is not conducive to the formation of vesicles[36–39]. Specifically, previous laboratory work has shown that strongly alkaline pH, high temperatures, ocean salinity and abundant divalent cations all disrupt the formation of vesicles from SCAs[36–40]. The conclusion that amphiphilic compounds "do not assemble into vesicles in seawater" might seem

[1]Centre for Life's Origins and Evolution, Department of Genetics, Evolution and Environment, University College London, London, UK. [2]Institute of Structural and Molecular Biology, Birkbeck College, London, UK. [3]Institute of Structural and Molecular Biology, University College London, London, UK. *e-mail: nick.lane@ucl.ac.uk

fatal to the idea that life originated in deep-sea hydrothermal vents[40]. Yet this conclusion is based on vesicles composed of decanoic acid or simple mixtures of two or three amphiphiles. Mixtures of SCAs with more complex head groups (such as amine, glycerol and sulfate) have been shown to form vesicles over a wider pH range, albeit predominantly at neutral and acidic pH (refs. [41,42]). The addition of 1-alkanols can stabilize fatty acid vesicles at the high pH found in alkaline vents[43,44]. Vesicles composed of decylamine and decanoic acid are stable even at pH 11 in the presence of some salts, but they produce curious crystalline aggregates between pH 2 and 10, while their prebiotic provenance is uncertain[45]. Polyaromatic hydrocarbons seem to improve vesicle stability further, although they have little congruence with modern membranes[45,46]. Yet despite these various indications that mixtures of amphiphiles can enhance vesicle stability, the combination of strongly alkaline pH, high temperatures, high salinity and abundant divalent cations is still often cited as an insuperable barrier to life beginning in oceanic hydrothermal systems[36–40]. We have therefore explored the properties of vesicles assembled from mixtures of the 6–12 most abundant SCAs formed through hydrothermal Fischer–Tropsch-type synthesis[21], combined with two simple isoprenoid molecules. Far from precluding vesicle formation at the origin of life, we show that alkaline hydrothermal conditions in fact promote vesicle assembly from these prebiotically plausible mixtures of amphiphiles.

Results

A 50 mM solution of pure decanoic acid vesicles (one of the most widely investigated vesicle-forming SCAs in origin-of-life research) was first tested to ensure that the methods employed here yielded results matching literature values. These results provided a transition point of pH ~7.2 and a range of vesicle formation of ~0.2 pH units, which is similar to previously reported values (Fig. 1)[47]. The first complex solution of vesicles that we investigated was a mixture of fatty acids from C_{10}–C_{15}, including both odd and even chain lengths (all of which are formed by Fischer–Tropsch-type synthesis under hydrothermal conditions), giving a total of six SCAs. A concentration of 5 mM (of each SCA) was used to test vesicle stability across a pH range of ~7 to 13. When fitted to a sigmoid curve (see the Supplementary Information) a transition point of pH ~8.45 was observed (Fig. 1). Confocal microscopy of the solution at this pH value confirmed the presence of vesicles (Fig. 1). A greater abundance of vesicles was observed at pH values below these transition points (Supplementary Figs. 1 and 2). The transition point appears to be a conservative estimate of the initiation point of vesicle formation, as confocal microscopy shows the presence of vesicles in mixed fatty acid solutions as high as pH ~9, whereas the observed transition point is pH ~8.5 (Supplementary Fig. 3).

Solutions containing fatty acids and 1-alkanols were prepared in molar ratios of 10:1, 5:1 and 1:1. The pH range of vesicle formation was unaffected by the addition of 1-alkanols in a 10:1 ratio, giving a transition point of pH ~8.5, similar to that of fatty acids alone (Extended Data Fig. 2). However, with a 5:1 ratio, the range was extended to a transition point of pH ~9.5 (Fig. 1). For a solution containing a 1:1 ratio of fatty acids to 1-alkanols, vesicle formation was observed from pH ~6.5 to 13 with no obvious transition point (Fig. 2a). Confocal microscopy confirms the presence of vesicles in solution across the entire pH range (Fig. 2). Encapsulation of the fluorescent dye pyranine clearly shows that these vesicles can trap and retain the dye (Fig. 3a) for periods of at least 24 h at pH 12 (Fig. 3b), confirming that they have an aqueous lumen and are stable over hours to days. Note that the fluorescence associated with vesicles after 24 h had fallen to 15–20% of that of fresh vesicles.

The CBC of the mixed fatty acid solution was determined to be 1.3 mM by optical density (OD) measurements (Fig. 4), with each SCA at a concentration of 225 μM. However, confocal microscopy at concentrations below 6 mM (combined SCA) did not reveal any vesicles in these solutions. We hypothesized that at lower concentrations vesicles are smaller in size than those at higher concentrations. To test this, cryogenic transmission electron microscopy (cryo-TEM) analysis was conducted on mixed fatty acid solutions below 6 mM concentration (with individual SCA concentrations of 100, 200, 300, 400 and 500 μM). These results showed that vesicles did in fact form in solutions as low as 600 μM total concentration but they were less than 200 nm in diameter, lower than the resolution limit of the confocal microscope (Fig. 4). These tiny vesicles do appear to have bounding membranes on cryo-TEM, although their appearance is equivocal, and it is possible that they are lipid droplets. Nonetheless, negative-staining transmission electron microscopy (NS-TEM) shows unequivocal evidence of the collapsed doughnut shapes associated with vesicles, on an equivalent scale (Extended Data Figs. 3 and 4). We therefore think it most likely that low concentrations of SCAs do simply produce smaller vesicles. These small vesicles were present in higher-concentration solutions as well and are probably present at most concentrations tested, but are simply not observable under a confocal microscope. If so, then the CBC determined by the OD analysis is a conservative estimate of the minimum SCA concentration required for vesicle formation, as OD measurements are diffraction-limited in the same way as confocal microscopy. CBC values for the 5:1 and 1:1 solutions were similar to those of fatty acids alone, and vesicles probably form below this concentration in these solutions as well (Extended Data Fig. 5).

Due to the extremely wide pH range of vesicle formation observed for 5 mM 1:1 solutions, this model was selected for further testing under the influence of salinity and divalent cations. Solutions were prepared in a range of conditions and analysed by confocal microscopy, cryo-TEM, NS-TEM and pyranine encapsulation. Modern day seawater contains on average 600 mM NaCl, 50 mM Mg^{2+} and 10 mM Ca^{2+}. These values are frequently cited as precluding the assembly of SCA vesicles, excluding any oceanic environment as a potential location for the origin of life[39,40]. As such, these concentrations were employed as the maximum concentrations for our experiments on the effects of salinity and divalent cations on vesicle formation, up to an ionic strength in the full salt mixture of 1.022 M (Supplementary Table 1). Vesicles were prepared in a range of 100–600 mM NaCl at pH ~9 and 12 and were observed in all solutions at pH ~12 (Fig. 5, Extended Data Fig. 6 and Supplementary Fig. 4). Vesicles were prepared from 10–50 mM $MgCl_2$ and 1–10 mM $CaCl_2$ at pH ~7, 9 and 12. Again, vesicle formation was observed at all concentrations at pH ~12 (Fig. 5, Extended Data Figs. 7 and 8 and Supplementary Figs. 5 and 6) but no vesicles were observed at pH 7 or 9 in the presence of 20 mM $MgCl_2$ or 5 mM $CaCl_2$ (Supplementary Fig. 7), so we did not test higher concentrations. Vesicles were formed at lower concentrations of salt and divalent cations below pH 12. Vesicles could also form long filaments, seen by both confocal microscopy and NS-TEM. While their structure was unclear by confocal microscopy, the filaments appeared to be composed of chains of individual vesicles by NS-TEM (Fig. 6). Note that vesicles burst under vacuum and so appear collapsed during microscopy.

Finally, 5 mM 1:1 fatty acid/1-alkanol vesicles were prepared in an alkaline (pH > 12) solution containing a combination of NaCl, Mg^{2+} and Ca^{2+} at modern seawater concentrations, thereby providing a more realistic analogue environment. Under these conditions, individual vesicles were not formed, and aggregates of vesicles were the predominant structures seen. It should be noted that cooling of vesicle solutions has been shown to lead to aggregation[40]. As the microscope stage used here was not heated, cooling of the solutions from their original 70 °C temperature may also have contributed to this aggregation. This experiment was repeated with the addition of equimolar amounts of two C_{10} isoprenoids, geranic acid and geraniol, which are prebiotically plausible molecules that are substantially under-researched in terms of their potential for prebiotic

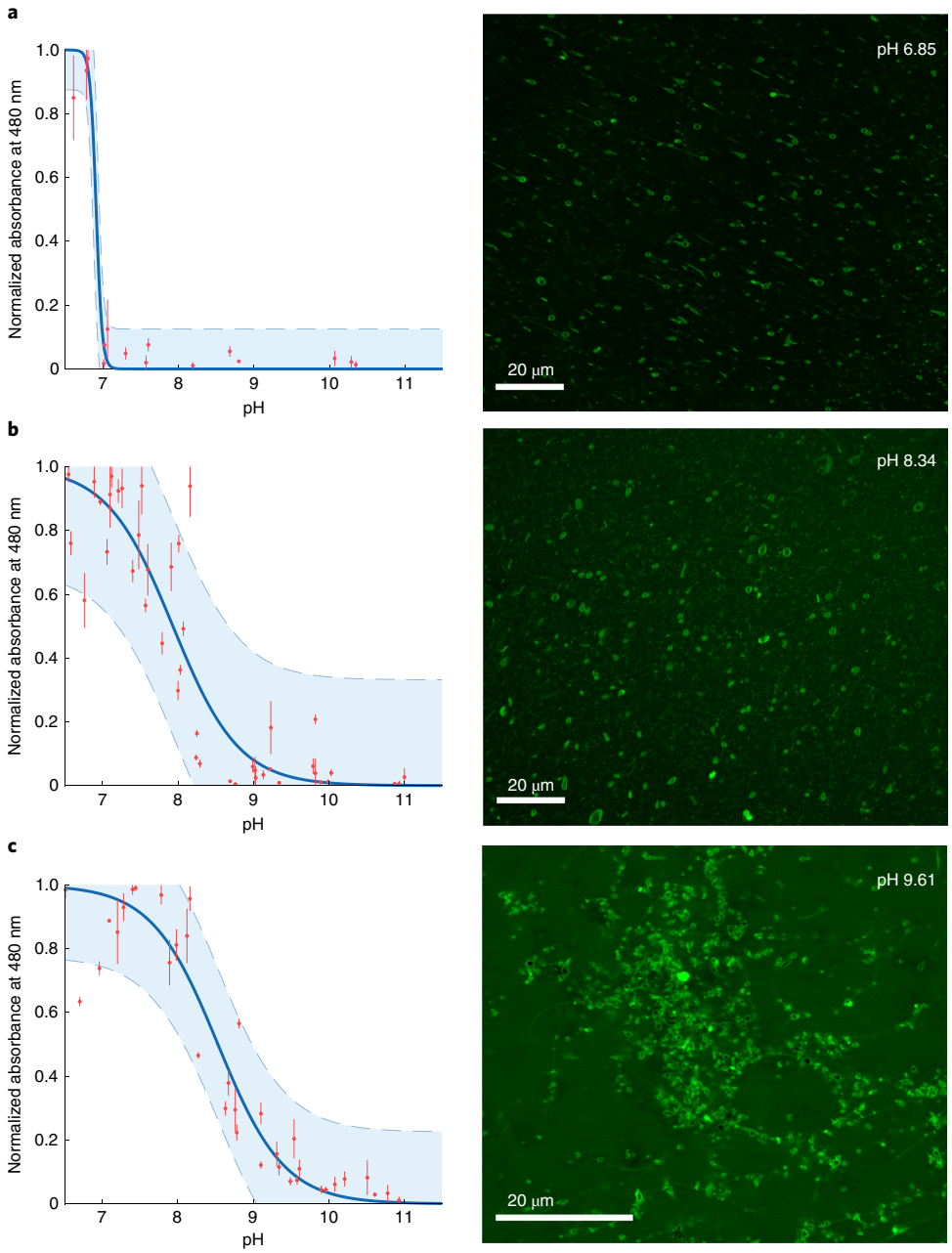

Fig. 1 | Mixtures of amphiphiles increase the pH range of vesicle formation. a–c, Plots of normalized absorbance at 480 nm versus pH, with corresponding confocal micrographs for the transition point from the micellar to vesicular phase, for 50 mM C_{10} fatty acid (**a**), 5 mM C_{10}–C_{15} fatty acid mixture (**b**) and 5 mM 5:1 C_{10}–C_{15} fatty acid/1-alkanol mixture (**c**). Error bars represent the standard deviation ($n = 3$). The data are fit to a sigmoid model (see Supplementary Information) represented by the solid blue line. Light blue shading indicates the 95% confidence interval.

vesicle formation. The inclusion of these two compounds enabled the formation of vesicles in an alkaline solution (pH ~12) containing a combination of 600 mM NaCl, 50 mM Mg^{2+} and 10 mM Ca^{2+} observed by confocal microscopy and cryo-TEM (Fig. 7) and confirmed by NS-TEM (Extended Data Fig. 9 and Supplementary Figs. 8–10).

To demonstrate that the vesicles observed independently by several different types of microscopy are indeed stable vesicles with a lumen, we examined their encapsulation of pyranine. Figure 3c shows that vesicles composed of the full amphiphile mix can encapsulate pyranine in water, while Fig. 3d shows that the dye is retained over at least 24 h, demonstrating the stability of these vesicles. However, encapsulation experiments are more problematic under high-salt conditions, especially in the presence of divalent cations, as most dyes, including the standards normally used for vesicle work, pyranine and calcein, interact with divalent cations or precipitate as hydroxides[48,49] (Supplementary Fig. 11). Control preparations of pyranine in water with or without salts (that is, with no SCAs present) show that pyranine fluorescence is largely suppressed in the presence of salts (Fig. 3e). Despite these issues, by preparing vesicles in the presence of pyranine, and adding a double-concentration salt mixture to achieve the required total salt concentration after encapsulation, we were able to demonstrate that 1:1:1 mixtures of all SCAs can indeed form stable vesicles capable of encapsulating the dye in alkaline solution (pH 12) containing a combination of 600 mM NaCl, 50 mM Mg^{2+} and 10 mM Ca^{2+} (Fig. 3f). We note

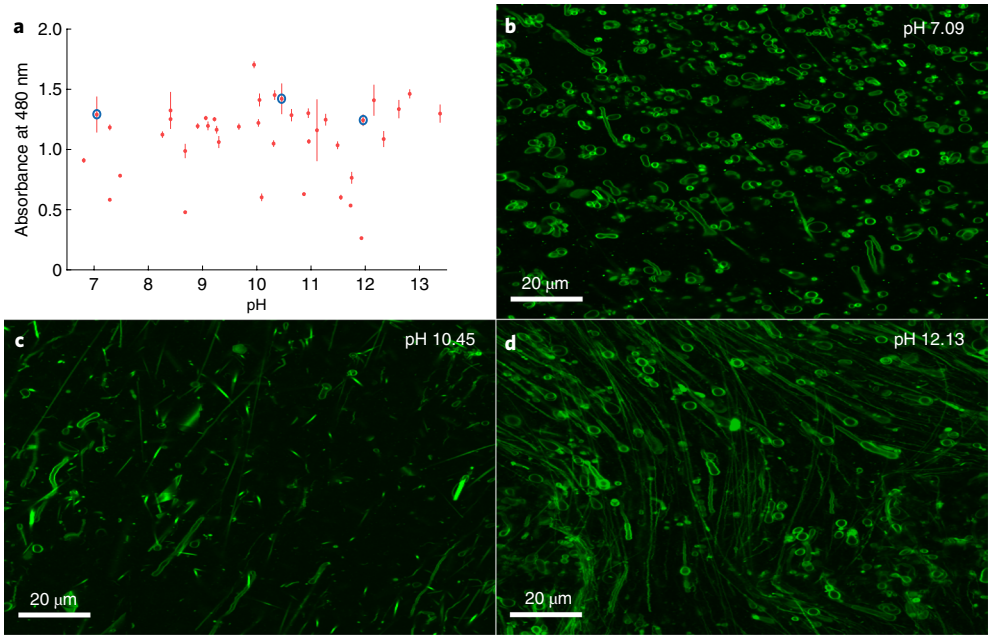

Fig. 2 | Fatty acid/1-alkanol mixtures form vesicles from pH 7 to pH 12. a–d, Plot of absorbance at 480 nm versus pH for 5 mM 1:1 C_{10}–C_{15} fatty acid/1-alkanol mixture (**a**) with corresponding confocal micrographs at pH 7.09 (**b**), pH 10.45 (**c**) and pH 12.13 (**d**). Error bars represent the standard deviation ($n = 3$).

that these vesicles are able to retain the dye despite the osmotic shock of being added to double-strength full salt mixtures. We also achieved encapsulation with calcein, despite interactions with salts (Extended Data Fig. 10). These findings confirm the cryo-TEM, confocal microscopy and NS-TEM, demonstrating that vesicles are indeed formed under oceanic alkaline hydrothermal conditions.

Discussion

Our results show that mixtures of 6–14 SCAs, including fatty acids, 1-alkanols and isoprenoids, can form stable vesicles in aqueous solution across a pH range of ~6 units from pH ~6.5 to >12. We have demonstrated vesicle stability under these conditions by encapsulation of the fluorescent dye pyranine over 24 h (Fig. 3) and shown the presence of vesicles by multiple methodologically wholly distinct techniques, including cryo-TEM, NS-TEM, confocal microscopy, ultraviolet–visible (UV-vis) and fluorescence spectroscopy. Warm (70 °C), alkaline (pH 12) solutions equivalent to those found in modern alkaline hydrothermal vents[34,50,51] actively promote vesicle formation and mitigate the interference produced by high concentrations of NaCl, Mg^{2+} and Ca^{2+}. In Hadean deep-ocean alkaline hydrothermal systems, vesicles should have formed readily from mixtures of prebiotic SCAs, probably produced by Fischer–Tropsch-type synthesis[21], giving rise to protocells at the origin of life.

Hydrothermal Fischer–Tropsch-type synthesis has been shown to form complex mixtures of fatty acids and 1-alkanols, as well as long-chain alkanes and alkenes, which decrease in their abundance with chain lengths above ~15 carbons[21]. We therefore used mixtures of these SCAs with chain lengths from C_{10}–C_{15}. Compared with the C_{10} decanoic acid, longer chain lengths lower the CBC by promoting more interactions between hydrophobic tails[52,53], effectively decreasing fatty acid solubility. Mixtures of fatty acids and 1-alkanols decrease the CBC still further, presumably through hydrogen bonding between the carboxylate and alcohol head gro ups[37,38,41,54]. Vesicles assembled from decanoic acid alone have a CBC of 39 mM, whereas mixtures of 12 C_{10}–C_{15} fatty acids and 1-alkanols (1:1) have a CBC around 30-fold lower, at 1.3 mM, with a concentration of 225 μM for each individual SCA. In fact, we found plentiful very small (<200 nm diameter) vesicles by NS-TEM and cryo-TEM at even lower concentrations (100 μM for each SCA; Fig. 4). In vents, a combination of hydrothermal Fischer–Tropsch-type synthesis (producing complex mixtures of SCAs with low CBCs[21]) with thermophoresis (concentrating SCAs above the CBC via thermal currents[25,26]) and interactions with mineral surfaces (enhancing vesicle assembly[27]) should promote vesicle formation even at very low SCA concentrations.

More complex SCA mixtures dramatically increase vesicle assembly under strongly alkaline conditions. Raising the number of fatty acids in solution from one to six expands the pH range of vesicle formation nearly 100-fold, from about 0.2 to almost 2 pH units (Fig. 1). Increasing the content of 1-alkanols elicits an even greater effect. In 1:1 mixtures with fatty acids, 1-alkanols produce stable vesicles above pH 12, as seen from the OD data, confocal images (Fig. 2) and encapsulation of the fluorescent dye pyranine over 24 h (Fig. 3). Vesicles form when amphiphiles are in solution at a pH close to their pK_a, the point at which their carboxylic acid headgroups exist equally in both protonated and deprotonated forms[55]. Hydrogen bonding between protonated and deprotonated head groups stabilizes bilayer structures. In contrast, protonation under acidic conditions promotes the formation of droplets, whereas deprotonation in alkaline conditions dissolves fatty acids or promotes micelle formation. Under alkaline hydrothermal conditions, fatty acids are well above their pK_a, hence all carboxylic acid head groups deprotonate, favouring dissolution[47]. Lengthening the fatty acid chains raises the apparent pK_a through hydrophobic interactions between their tails[52,53], but this effect is limited. Adding 1-alkanols strongly promotes vesicle formation as the alcohol head groups do not deprotonate[37,55]. A 1:1 mixture of fatty acids and 1-alkanols therefore forms vesicles at high pH as the head groups of the two species are equally protonated and deprotonated, forming stable hydrogen bonds even in strongly alkaline conditions (Fig. 2).

The standard laboratory procedure to promote vesicle self-assembly begins with deprotonated fatty acids at high pH, to ensure that amphiphiles are in solution or micellar form[47]. The pH is then titrated down to the apparent pK_a, whereupon vesicles

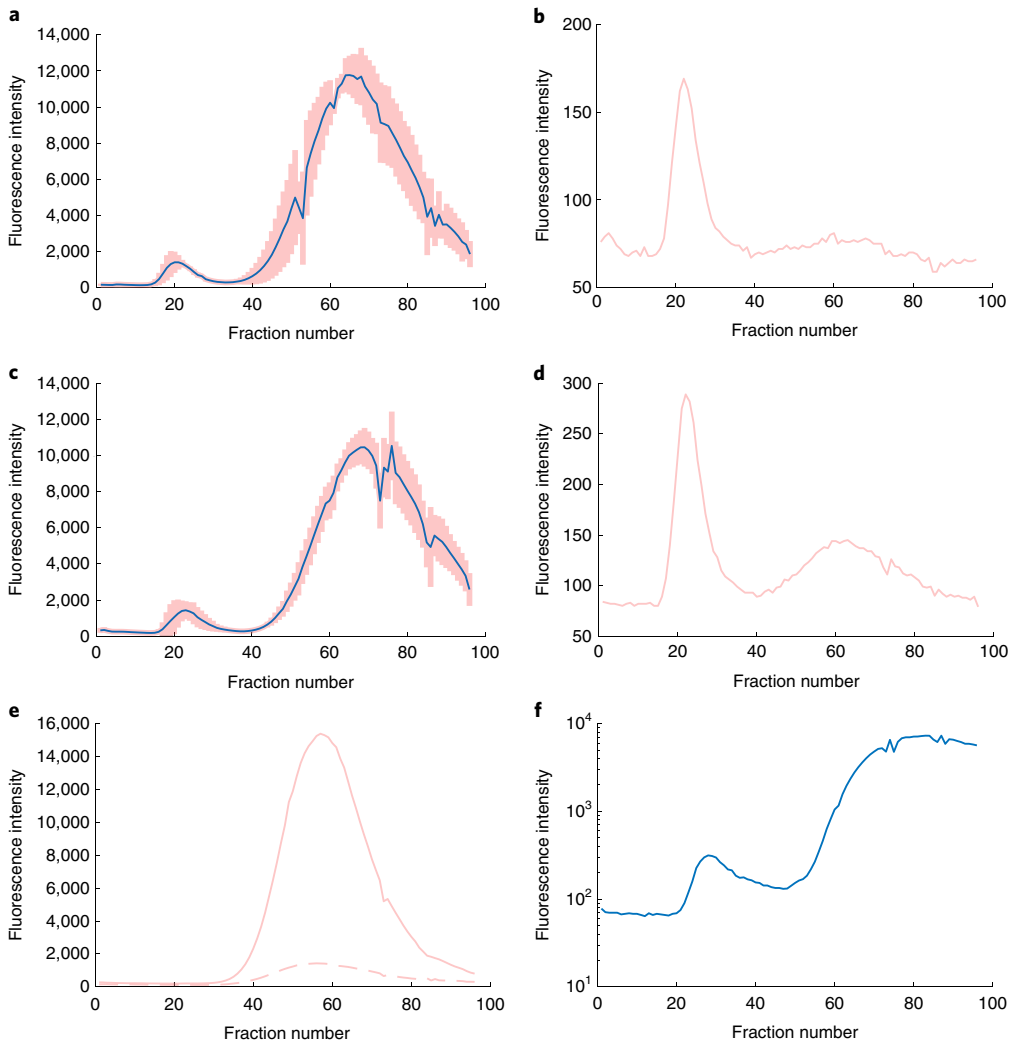

Fig. 3 | Encapsulation of fluorescent dyes confirms stable vesicle formation. a, Encapsulation of the fluorescent dye pyranine, showing a peak for pyranine encapsulated within vesicles composed of 5 mM 1:1 C_{10}–C_{15} fatty acid/1-alkanol mixture at fraction number ~20, and a larger peak for free dye at fraction number ~70. **b**, Vesicles as in **a** but after 24 h encapsulation, with ~20% of the encapsulated pyranine peak remaining at fraction number ~20. **c**,**d**, Equivalent plots for the full 5 mM 1:1:1 C_{10}–C_{15} fatty acid/1-alkanol/C_{10} isoprenoid mixture, displaying initial pyranine encapsulation (**c**) and encapsulation after 24 h (**d**). **e**, Fluorescence from free pyranine in water (solid line) and water with full salt solution at pH 12 (dashed line), showing interaction of dye with salt mixture leading to a substantially lower free pyranine peak after chromatography. **f**, Encapsulation of pyranine in vesicles composed of 5 mM 1:1:1 C_{10}–C_{15} fatty acid/1-alkanol/C_{10} isoprenoid mixture, with encapsulated pyranine fluorescence at fraction number ~20 and free dye at fraction number ~70. Note log scale on *y* axis to emphasize encapsulation despite disruption from salt interactions. Pink shading in **a** and **c** represents the standard deviation ($n = 3$).

self-assemble. In other words, vesicles do not form spontaneously at lower pH, but initially require strongly alkaline pH to self-assemble. While it is possible to form vesicles without raising the pH, we note that this can be achieved only after adding NaOH in the presence of buffer. In the absence of buffers, alkaline conditions are necessary to first deprotonate and dissolve fatty acids. We have observed that simply adding SCAs to salty water at pH 7 does not form vesicles, as the fatty acids are mostly protonated and form an emulsion of lipid droplets rather than bilayer vesicles. Once fatty acids are deprotonated and dissolved under alkaline conditions, titration down to more acidic conditions, as in the laboratory procedure, now forms bilayer vesicles. This titration would occur naturally by mixing with mildly acidic ocean waters in Hadean vents[56], and does not disassemble vesicles except at pH below 6.5 (though earlier work shows that vesicles can also form even at strongly acidic pH (refs. [42,45])). With more complex mixtures of fatty acids and 1-alkanols, there is no need to titrate with acid to form vesicles, as they form spontaneously even above pH 12, in the absence of salts. Initial heating is needed for similar reasons. Vesicles do not form readily from solid fatty acids below their melting point (or when protonated, as noted above). The melting point of fatty acids and 1-alkanols depends on chain length, with the C_{15} fatty acid melting around 53 °C. To dissolve long-chain SCAs therefore requires temperatures similar to those found in alkaline hydrothermal vents (typically 50–90 °C)[34,50,51]; we used 70 °C. Once formed at warm temperatures, vesicles are still present on cooling (Supplementary Fig. 12), again consistent with mixing in the vents with cooler ocean waters. Far from precluding protocell formation, the pH and temperature range in alkaline hydrothermal vents should therefore promote their self-assembly at the origin of life.

Salinity is also known to promote vesicle assembly through both polar (electrical shielding of the charged head groups) and

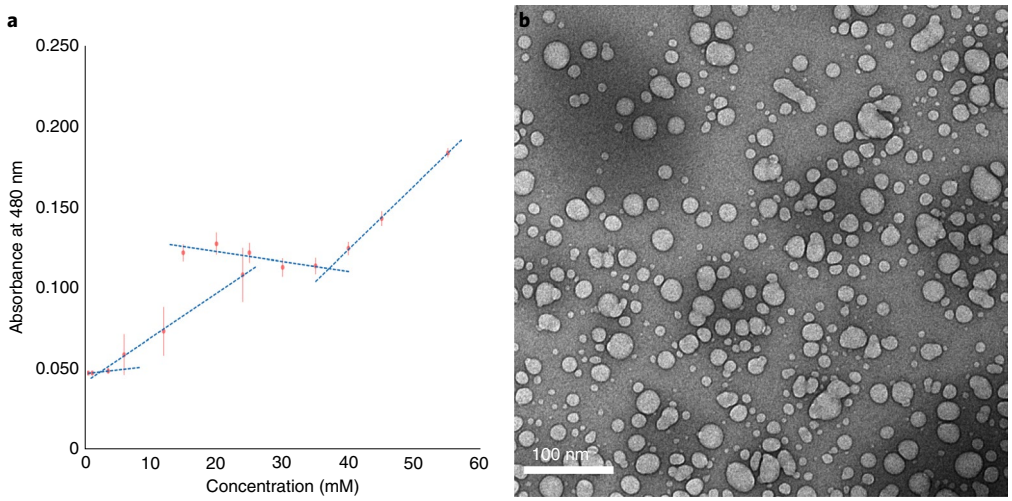

Fig. 4 | Mixtures of amphiphiles lower the concentration needed to form vesicles by ~30-fold. a, Plot of absorbance at 480 nm versus concentration for C_{10}–C_{15} fatty acid mixture at pH ~8 and C_{10} fatty acid at pH ~7 showing calculated CBCs of 1.35 mM (with each individual fatty acid present at 225 μM) and 39 mM, respectively. Error bars represent the standard deviation ($n = 3$). Dashed blue lines indicate linear fits to each dataset. **b**, Cryo-TEM micrograph of 600 μM 1:1 C_{10}–C_{15} fatty acid/1-alkanol mixture at pH 7.71 (with each individual fatty acid present at 100 μM).

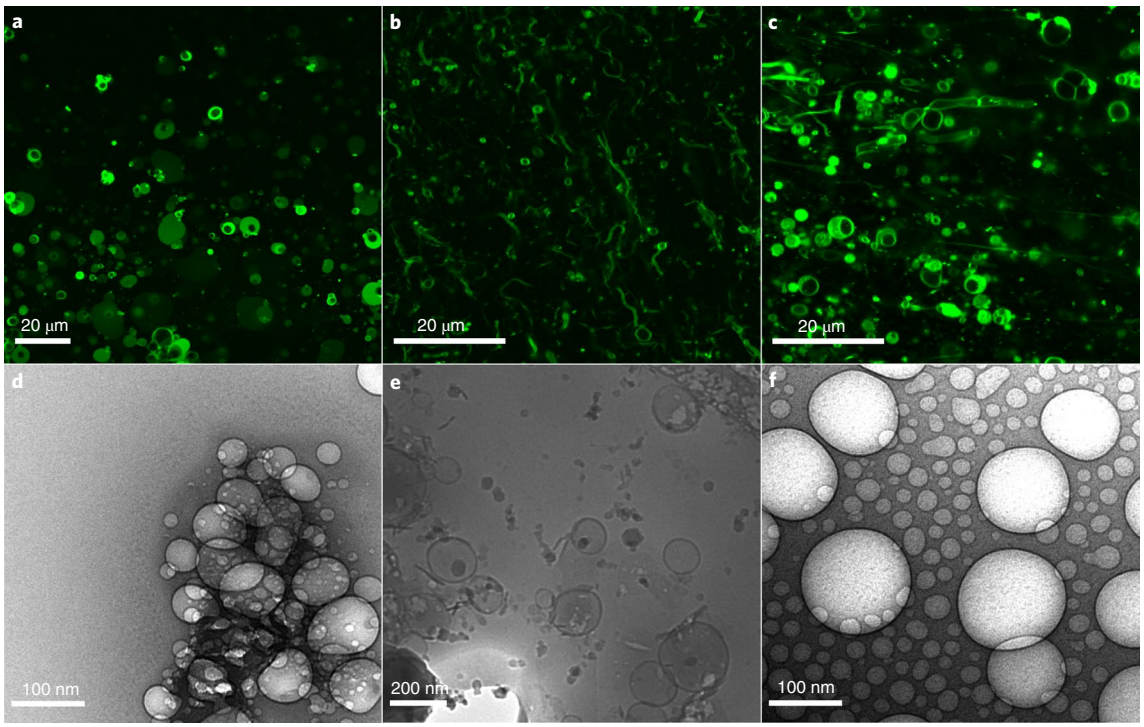

Fig. 5 | Fatty acid/1-alkanol mixtures form vesicles in the presence of salt and divalent cations. a–**f**, Confocal micrographs of 5 mM 1:1 C_{10}–C_{15} fatty acid/1-alkanol mixture in 600 mM NaCl pH 11.17 (**a**), 50 mM $MgCl_2$ pH 11.65 (**b**) and 10 mM $CaCl_2$ pH 11.84 (**c**) along with corresponding cryo-TEM micrographs at pH 12.17 (**d**), pH 12.31 (**e**) and pH 12.29 (**f**).

non-polar (more pronounced phase partitioning of hydrophobic tails) effects[42,54]. Nonetheless, earlier work concluded that high-salt concentrations (>150 mM) disrupt vesicle formation and would preclude the formation of protocells at modern ocean salinity (~600 mM NaCl)[37–41]. If the salinity of Hadean oceans were equivalent, this reasoning goes, then life could not have begun in the oceans and must have started in terrestrial freshwater pools. The inferred salinity of Hadean oceans is difficult to constrain. Extrapolations based on fluid inclusions trapped in ancient rocks are questionable[57], but three factors are pertinent: (1) acid leaching of the crust by hot early oceans should have released Na^+ into the oceans rapidly, so that maximum salinity was reached quickly[57]; (2) the lack of evaporitic salt deposits in the Hadean, given practically global oceans, means that Hadean oceans could have had nearly double the salt content of modern oceans[58]; but (3) the sequestration of water as hydrated minerals (for example, serpentinites) over 4.5 billion years means that Hadean oceans could have had twice the volume of modern oceans[59–61]. A conservative position is therefore

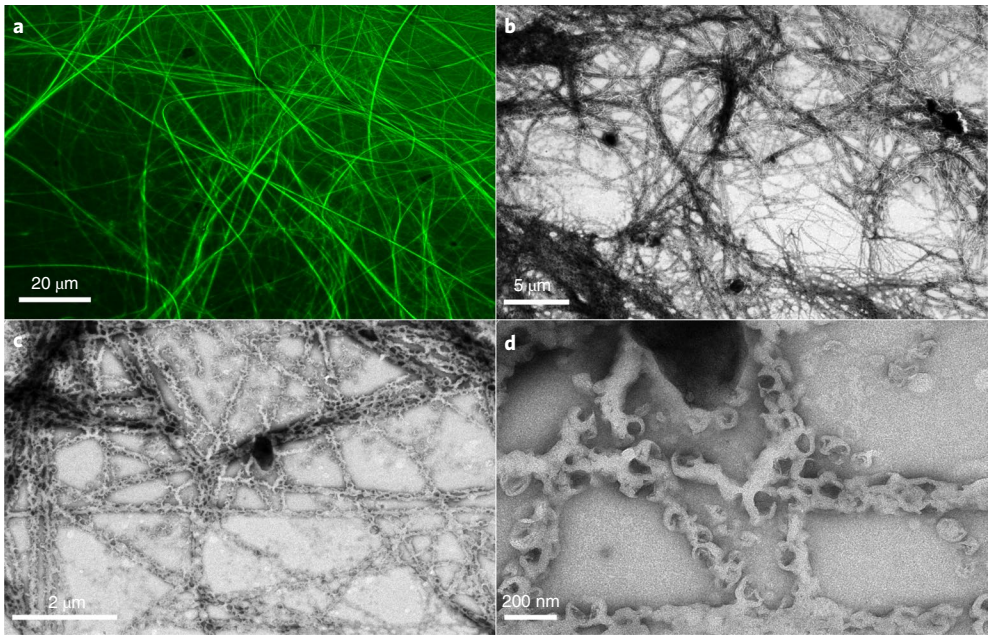

Fig. 6 | Salts can promote the formation of filaments composed of vesicles formed from mixed amphiphiles. a–d, Filamentous vesicle aggregates formed in a solution of 5 mM C_{10}–C_{15} fatty acids in 100 mM NaCl as observed by confocal microscopy (**a**) and NS-TEM (**b**–**d**). During NS-TEM, vesicles burst under vacuum leading to collapsed structures as seen in these micrographs.

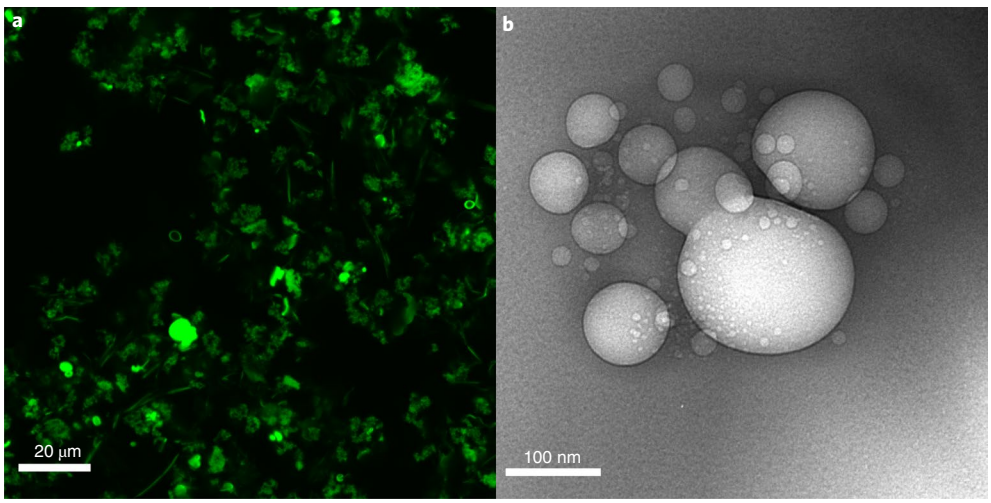

Fig. 7 | Mixtures of amphiphiles support vesicle formation under oceanic alkaline hydrothermal conditions. a,**b**, Confocal (**a**) and cryo-TEM (**b**) micrographs of 5 mM 1:1:1 C_{10}–C_{15} fatty acid/1-alkanol/C_{10} isoprenoid mixture in a combined solution of 600 mM NaCl, 50 mM $MgCl_2$ and 10 mM $CaCl_2$ at pH 12.69 and 11.75, respectively.

that ocean salinity was similar to today. If life started in the oceans, then protocells would need to tolerate ~600 mM NaCl.

The difficulty of forming vesicles at modern ocean salinity reported by others can best be ascribed to the use of simple mixtures of largely C_{10} SCAs. We show that more complex mixtures of 12 C_{10}–C_{15} fatty acids and 1-alkanols do indeed form numerous individual vesicles at modern ocean salinity (Fig. 5). Higher salinity sometimes promotes the aggregation of vesicles or the formation of filamentous structures observed by confocal microscopy (Fig. 6), and certainly there are fewer individual vesicles under these conditions. However, NS-TEM analysis suggests that these filaments are composed entirely of individual SCA vesicles (Fig. 6). The vesicles burst under vacuum, so appear collapsed during microscopy. Similar structures have been found in liposome research previously (by both confocal microscopy and NS-TEM, as reported here) and are known to be metastable[62–64]. More work is needed to characterize these remarkable structures and elucidate their chemical properties in an origin-of-life context.

Divalent cations, notably Mg^{2+} and Ca^{2+}, have also been shown to disrupt vesicle formation[39,40]. Their concentration in Hadean oceans is unknown, and estimates vary greatly[65,66]. Ocean levels are in any case a poor surrogate for vent systems; the concentration of Ca^{2+} and Mg^{2+} in modern alkaline vent fluids is extremely variable, with some features containing no Ca^{2+} or Mg^{2+} at all[67]. We therefore examined vesicle stability in the presence of modern seawater concentrations of Mg^{2+} and Ca^{2+}, as earlier work reported that sea-

water levels aggregate fatty acid/1-alkanol vesicles into insoluble curds[39,40]. While simple organic chelators such as citrate can prevent this from happening[68] (and vesicles composed of decylamine and decanoic acid have been shown to form in the presence of 0.1 M Mg^{2+} and Ca^{2+} salts[44]), we find that alkaline pH alone offers some protection. Divalent cations form complexes with amphiphile head groups at low pH, prohibiting bilayer formation and producing soapy solutions[36–41,47,55]. In contrast, strongly alkaline conditions favour hydroxide complexes with these inorganic ions, in effect rendering them unavailable for vesicle disruption. Plentiful vesicles form at strongly alkaline pH (pH 11–12) in the presence of 50 mM Mg^{2+} and 10 mM Ca^{2+} (Fig. 5) but very few form at pH < 9 (Supplementary Fig. 7). While the combination of modern seawater concentrations of NaCl, Mg^{2+} and Ca^{2+} at pH 11 and 70 °C did disrupt vesicle formation with mixtures of 12 C_{10}–C_{15} fatty acids and 1-alkanols, addition of two C_{10} isoprenoids, geranic acid and geraniol, enabled vesicle assembly even under these most extreme conditions, as demonstrated by confocal microscopy, cryo-TEM (Fig. 7) and NS-TEM (Extended Data Fig. 9 and Supplementary Figs. 8–10). We confirmed the stability of these vesicles in oceanic alkaline hydrothermal conditions through encapsulation of the fluorescent dye pyranine (Fig. 3). We explore the reasons for this increased stability elsewhere[69].

We conclude that deep-sea alkaline hydrothermal conditions in the Hadean should have promoted the synthesis of long-chain amphiphiles and their self-assembly into protocells at the origin of life. Thermophoresis[26] and interactions with mineral surfaces in porous vents[27] concentrate amphiphiles above the CBC. Vents sustain the moderately high temperatures needed to ensure that longer-chain amphiphiles are above their melting point and so available for vesicle formation in solution[41]. Alkaline pH is essential to dissolve the SCAs in water, deprotonating the head groups of some amphiphiles and reducing the concentration of divalent cations such as Ca^{2+} and Mg^{2+} in solution. Titration by mixing with more acidic ocean waters within vents favours vesicle self-assembly. Salts promote vesicle assembly[41] as well as aggregation of three-dimensional structures that could potentially harness geologically sustained pH gradients to drive CO_2 fixation[29,70,71]. Mixtures of amphiphiles are geochemically[21] and biochemically[72] meaningful, and are critical to forming protocells capable of growth and simple heredity[29] at the origin of life.

Methods

Materials. Decanoic acid, dodecanoic acid, tetradecanoic acid, decan-1-ol, undecan-1-ol and geraniol were purchased from Acros Organics. Undecanoic acid, tridecanoic acid, tridecan-1-ol, geranic acid, sodium chloride (NaCl), calcium chloride dihydrate ($CaCl_2{\cdot}2H_2O$), Sephadex G-50 and 8-hydroxypyrene-1,3,6-trisulfonic acid (pyranine) were purchased from Sigma Aldrich. Pentadecanoic acid, dodecan-1-ol, tetradecan-1-ol, pentadecan-1-ol and magnesium chloride hexahydrate ($MgCl_2{\cdot}6H_2O$) were purchased from Alfa Aesar. All reagents used were analytical grade (≥97%).

Preparation of vesicle solutions. All laboratory work was carried out in a dry heat block (SciQuip HP120-S) at 70 °C. Density values for each compound at this temperature were obtained gravimetrically (Supplementary Table 2). Vesicle solutions were prepared daily following a modified version of the procedure outlined by Monnard and Deamer[47]. Buffers were not employed in any solutions in an effort to maintain prebiotic relevance. A 7 ml 10 mM stock solution of vesicles was prepared by adding equimolar concentrations of each fatty acid to 4 ml deionized H_2O in a glass vial. The pH was adjusted to >12 with 500 µl 1 M NaOH and the solution was vortexed to ensure full dissolution of deprotonated acids. For vesicles containing 1-alkanols, equimolar concentrations were added at this stage and the solution was vortexed. The solution was then brought to a final volume of 7 ml with 1 M NaOH (final pH ~12). Then, 500 µl of the stock solution was added to a fresh glass vial. The solution was titrated with gradual addition of 1 M HCl followed by pH measurement (Fisher Scientific accumet AE150 meter with VWR semi-micro pH electrode) to achieve the desired pH. The solution was brought to a final volume of 1 ml with deionized H_2O resulting in a concentration of 5 mM, after which the pH value was recorded. For isoprenoid-containing solutions, isoprenoid acids and alcohols were added in conjunction with fatty acids and 1-alkanols, respectively.

For CBC experiments, the same procedure was used followed by serial dilution to obtain the desired concentrations. The pH of each solution was measured again before analysis. To test the influence of NaCl, Mg^{2+} and Ca^{2+}, this procedure was carried out using aqueous solutions of the desired salt concentration in the place of H_2O. Identical quantities of salts were dissolved in 1 M NaOH and 1 M HCl for use in pH adjustment, thereby ensuring that the concentration of salt remained constant throughout the experiment.

Determination of vesicle formation and CBC. OD measurements were obtained by measuring absorbance at 480 nm on an Infinite M200 Pro Spectrophotometer (Tecan) and data were processed using the Magellan software package. Three 50 µl aliquots of each solution were transferred to separate wells on a Falcon black 96-well plate (preheated to 70 °C) and immediately analysed. The instrument was set to 30 °C and the plate was shaken for 10 s before analysis. To determine the pH range of vesicle formation, data from multiple solutions were collated and a plot of pH versus absorbance was prepared. Minimal OD values indicate the presence of micelles. As the SCAs are gradually protonated, vesicles begin to form and the OD increases. Maximum values are obtained once SCAs become fully protonated and begin to form droplets as opposed to vesicles (Extended Data Fig. 1). To allow for better data visualization and comparison, values in Fig. 1 were normalized and fit to a sigmoid model representing the phase transition of the solutions. The initial upward turning point of the curve was defined as the transition point whereby vesicle formation begins. Interpretations made based on these plots were confirmed by confocal and electron microscopy.

CBC was also determined by OD measurement. Solutions were prepared in a range of concentrations and analysed as previously described. Data were interpreted following the same procedure as Maurer and Nguyen[54]. A linear function was fit through baseline values and through increasing values. The point of intersection of these two lines corresponds to the CBC and was determined algebraically.

Encapsulation and release of pyranine dye. Encapsulation capacity of vesicles was determined by preparation of solutions in the presence of 10 µM pyranine dye. All solutions were maintained at 70 °C during the procedure. A 200 µl aliquot of the solution was then separated by size exclusion chromatography using a glass column (30 × 1 cm^2) filled with Sephadex G-50 medium beads. Fractions (three drops, ~130 µl total) were collected in a Falcon black 96-well plate and analysed immediately. Encapsulation was measured by fluorescence spectroscopy on an Infinite M200 Pro spectrophotometer (Tecan) using excitation and emission wavelengths of 450 and 508 nm, respectively. Data were processed using the Magellan software package. Vesicle fractions were combined and separated again by size exclusion chromatography after 24 h to determine release of pyranine over time.

Confocal microscopy. Confocal microscopy of vesicle solutions was performed on a Zeiss LSM-T-PMT with an Ar laser at 514 nm coupled to an Airyscan detector. First, 0.5 µl 100 µM rhodamine-6G was added to a heated glass slide, followed by 5 µl sample solution. These were mixed on the slide and covered with a heated coverslip. Images were captured using a ×63 oil objective.

NS-TEM. Samples were analysed by transmission electron microscopy (TEM) using an NS-TEM method. A drop of sample solution was applied to a copper TEM grid and allowed to stand for 1 min. Excess sample was removed by blotting with filter paper. An aliquot of 1.5% aqueous uranyl acetate solution was applied to the grid for a further 1 min and the excess was subsequently removed with filter paper. Samples were analysed immediately on a JEOL 1010 TEM.

Cryo-TEM. Samples were applied directly to glow-discharged Lacey Carbon (400 mesh Cu) grids (Agar Scientific) for 30 s, blotted for 8.5 or 11 s at 4.5 °C and 95% humidity, and then rapidly plunged into liquid ethane using a Vitrobot Mark IV (Thermo Fisher). Imaging was completed using a T10 microscope (FEI) operated at 100 kV. Images were collected at a magnification range of ×7,000 to ×34,000.

Reporting Summary. Further information on research design is available in the Nature Research Reporting Summary linked to this article.

Data availability

All data are available in the main text, Extended Data Figs. 1–10 and the Supplementary Information.

Received: 30 April 2019; Accepted: 25 September 2019;
Published online: 4 November 2019

References

1. Mitchell, P. in *The Origin of Life on the Earth* (eds Oparin, A. I. et al.) 437–443 (Pergamon Press, 1957).
2. Nitschke, W. & Russell, M. J. Hydrothermal focusing of chemical and chemiosmotic energy, supported by delivery of catalytic Fe, Ni, Mo/W, Co, S and Se, forced life to emerge. *J. Mol. Evol.* **69**, 481–496 (2009).

3. Fuchs, G. Alternative pathways of carbon dioxide fixation: insights into the early evolution of life? *Annu. Rev. Microbiol.* **65**, 631–658 (2011).
4. Lane, N. & Martin, W. F. The origin of membrane bioenergetics. *Cell* **151**, 1406–1416 (2012).
5. Mulkidjanian, A. Y., Galperin, M. Y. & Koonin, E. V. Co-evolution of primordial membranes and membrane proteins. *Trends Biochem. Sci.* **34**, 206–215 (2009).
6. Koga, Y., Kyuragi, T., Nishihara, M. & Sone, N. Did archaeal and bacterial cells arise independently from noncellular precursors? A hypothesis stating that the advent of membrane phospholipid with enantiomeric glycerophosphate backbones caused the separation of the two lines of descent. *J. Mol. Evol.* **46**, 54–63 (1998).
7. Martin, W. & Russell, M. J. On the origins of cells: a hypothesis for the evolutionary transitions from abiotic geochemistry to chemoautotrophic prokaryotes, and from prokaryotes to nucleated cells. *Phil. Trans. R. Soc. B* **358**, 59–85 (2003).
8. Koga, Y. Early evolution of membrane lipids: how did the lipid divide occur? *J. Mol. Evol.* **72**, 274–282 (2011).
9. Sojo, V. On the biogenic origins of homochirality. *Orig. Life Evol. Biosph.* **45**, 219–224 (2015).
10. Lombard, J., López-García, P. & Moreira, D. The early evolution of lipid membranes and the three domains of life. *Nat. Rev. Microbiol.* **10**, 507–515 (2012).
11. Shimada, H. & Yamagishi, A. Stability of heterochiral hybrid membrane made of bacterial sn-G3P lipids and archaeal sn-G1P lipids. *ACS Biochem.* **50**, 4114–4120 (2011).
12. Caforio, A., Siliakus, M. F., Exterkate, M., Jain, S. & Jumde, V. R. Converting *Escherichia coli* into an archaebacterium with a hybrid heterochiral membrane. *Proc. Natl Acad. Sci. USA* **115**, 3705–3709 (2018).
13. Hanczyc, M. M. & Szostak, J. W. Replicating vesicles as models of primitive cell growth and division. *Curr. Opin. Chem. Biol.* **8**, 660–664 (2004).
14. Chen, I. A. & Szostak, J. W. Membrane growth can generate a transmembrane pH gradient in fatty acid vesicles. *Proc. Natl Acad. Sci. USA* **101**, 7965–7970 (2004).
15. Chen, I. A. & Szostak, J. W. A kinetic study of the growth of fatty acid vesicles. *Biophys. J.* **87**, 988–998 (2004).
16. Sojo, V., Pomiankowski, A. & Lane, N. A bioenergetic basis for membrane divergence in archaea and bacteria. *PLoS Biol.* **12**, e1001926 (2014).
17. Segré, D., Ben-Eli, D., Deamer, D. W. & Lancet, D. The lipid world. *Orig. Life Evol. Biosph.* **31**, 119–145 (2001).
18. Segré, D., Ben-Eli, D. & Lancet, D. Compositional genomes: prebiotic information transfer in mutually catalytic noncovalent assemblies. *Proc. Natl Acad. Sci. USA* **97**, 4112–4117 (2000).
19. Amend, J. P. & McCollom, T. M. Energetics of biomolecule synthesis on early earth. *ACS Symp. Ser.* **1025**, 63–94 (2009).
20. Martin, W. Carbon–metal bonds: rare and primordial in metabolism. *Trends Biochem. Sci.* **44**, 807–818 (2019).
21. McCollom, T. M., Ritter, G. & Simoneit, B. R. T. Lipid synthesis under hydrothermal conditions by Fischer-Tropsch reactions. *Orig. Life Evol. Biosph.* **29**, 153–166 (1999).
22. Scheidler, C., Sobotta, J., Eisenreich, W., Wächtershäuser, G. & Huber, C. Unsaturated $C_{3,5,7,9}$-monocarboxylic acids by aqueous, one-pot carbon fixation: possible relevance for the origin of life. *Sci. Rep.* **6**, 27595 (2016).
23. Decker, P. & Schweer, H. Reactions in the formol bioid: the origin of branched chains of isoprenoids, valine, and leucines. *Orig. Life* **14**, 335–342 (1984).
24. Pray, H. A., Schweickert, C. E. & Minnich, B. H. Solubility of hydrogen, oxygen, nitrogen, and helium in water at elevated temperatures. *Ind. Eng. Chem.* **44**, 1146–1151 (1952).
25. Baaske, P. et al. Extreme accumulation of nucleotides in simulated hydrothermal pore systems. *Proc. Natl Acad. Sci. USA* **104**, 9346–9351 (2007).
26. Budin, I., Bruckner, R. J. & Szostak, J. W. Formation of protocell-like vesicles in a thermal diffusion column. *J. Am. Chem. Soc.* **131**, 9628–9629 (2009).
27. Hanczyc, M. M., Mansy, S. S. & Szostak, J. W. Mineral surface directed membrane assembly. *Orig. Life Evol. Biosph.* **37**, 67–82 (2007).
28. Buckel, W. & Thauer, R. K. Flavin-based electron bifurcation, ferredoxin, flavodoxin, and anaerobic respiration with protons (Ech) or NAD^+ (Rnf) as electron acceptors: a historical review. *Front. Microbiol.* **9**, 401 (2018).
29. West, T., Sojo, V., Pomiankowski, A. & Lane, N. The origin of heredity in protocells. *Phil. Trans. R. Soc. B* **372**, 20160419 (2017).
30. Russell, M. J. & Hall, A. J. The emergence of life from iron monosulphide bubbles at a submarine hydrothermal redox and pH front. *J. Geol. Soc. London.* **154**, 377–402 (1997).
31. Russell, M. J. & Martin, W. The rocky roots of the acetyl-CoA pathway. *Trends Biochem. Sci.* **29**, 358–363 (2004).
32. Russell, M. J., Daniel, R. M., Hall, A. J. & Sherringham, J. A hydrothermally precipitated catalytic iron sulphide membrane as a first step toward life. *J. Mol. Evol.* **39**, 231–243 (1994).
33. Martin, W. & Russell, M. J. On the origin of biochemistry at an alkaline hydrothermal vent. *Phil. Trans. R. Soc. Lond. B* **362**, 1887–1925 (2007).
34. Martin, W., Baross, J., Kelley, D. & Russell, M. J. Hydrothermal vents and the origin of life. *Nat. Rev. Microbiol.* **6**, 805–814 (2008).
35. Russell, M. J. et al. The drive to life on wet and icy worlds. *Astrobiology* **14**, 308–343 (2014).
36. Monnard, P.-A., Apel, C. L., Kanavarioti, A. & Deamer, D. W. Influence of ionic inorganic solutes on self-assembly and polymerization processes related to early forms of life: implications for a prebiotic aqueous medium. *Astrobiology* **2**, 139–152 (2002).
37. Monnard, P. A. & Deamer, D. W. Membrane self-assembly processes: steps toward the first cellular life. *Anat. Rec.* **207**, 123–151 (2002).
38. Szostak, J. W., Bartel, D. P. & Luisi, P. L. Synthesizing life. *Nature* **409**, 387–390 (2001).
39. Deamer, D. The role of lipid membranes in life's origin. *Life* **7**, 5 (2017).
40. Milshteyn, D., Damer, B., Havig, J. & Deamer, D. Amphiphilic compounds assemble into membranous vesicles in hydrothermal hot spring water but not in seawater. *Life* **8**, 11 (2018).
41. Maurer, S. The impact of salts on single chain amphiphile membranes and implications for the location of the origin of life. *Life* **7**, 44 (2017).
42. Maurer, S. E. et al. Vesicle self-assembly of monoalkyl amphiphiles under the effects of high ionic strength, extreme pH, and high temperature environments. *Langmuir* **34**, 15560–15568 (2018).
43. Apel, C. L., Deamer, D. W. & Mautner, M. N. Self-assembled vesicles of monocarboxylic acids and alcohols: conditions for stability and for the encapsulation of biopolymers. *Biochim. Biophys. Acta* **1519**, 1–9 (2002).
44. Rendón, A. et al. Model systems of precursor cellular membranes: long-chain alcohols stabilize spontaneously formed oleic acid vesicles. *Biophys. J.* **102**, 278–286 (2012).
45. Namani, T. & Deamer, D. W. Stability of model membranes in extreme environments. *Orig. Life Evol. Biosph.* **38**, 329–341 (2008).
46. Cape, J. L., Monnard, P. A. & Boncella, J. M. Prebiotically relevant mixed fatty acid vesicles support anionic solute encapsulation and photochemically catalyzed trans-membrane charge transport. *Chem. Sci.* **2**, 661–671 (2011).
47. Monnard, P. A. & Deamer, D. W. Preparation of vesicles from nonphospholipid amphiphiles. *Methods Enzymol.* **372**, 133–151 (2003).
48. Thanh Thuy, D., Decnop-Weever, D., Th. Kok, W., Luan, P. & Vong Nghi, T. Determination of traces of calcium and magnesium in rare earth oxides by flow-injection analysis. *Anal. Chim. Acta* **295**, 151–157 (1994).
49. Avnir, Y. & Barenholz, Y. pH determination by pyranine: medium-related artifacts and their correction. *Anal. Biochem.* **347**, 34–41 (2005).
50. Kelley, D. S. et al. An off-axis hydrothermal vent field near the Mid-Atlantic Ridge at 30° N. *Nature* **412**, 145–149 (2001).
51. Kelley, D. S. et al. A serpentinite-hosted ecosystem: the Lost City hydrothermal field. *Science* **307**, 1428–1434 (2005).
52. Smith, R. & Tanford, C. Hydrophobicity of long chain *n*-alkyl carboxylic acids, as measured by their distribution between heptane and aqueous solutions. *Proc. Natl Acad. Sci. USA* **70**, 289–293 (1973).
53. Budin, I., Prywes, N., Zhang, N. & Szostak, J. W. Chain-length heterogeneity allows for the assembly of fatty acid vesicles in dilute solution. *Biophys. J.* **107**, 1582–1590 (2014).
54. Maurer, S. E. & Nguyen, G. Prebiotic vesicle formation and the necessity of salts. *Orig. Life Evol. Biosph.* **46**, 215–222 (2016).
55. Hargreaves, W. R. & Deamer, D. W. Liposomes from ionic, single-chain amphiphiles. *Biochemistry* **17**, 3759–3768 (1978).
56. Sojo, V., Herschy, B., Whicher, A., Camprubí, E. & Lane, N. The origin of life in alkaline hydrothermal vents. *Astrobiology* **16**, 181–197 (2016).
57. Marty, B., Avice, G., Bekaert, D. V. & Broadley, M. W. Salinity of the Archaean oceans from analysis of fluid inclusions in quartz. *C. R. Geosci.* **350**, 154–163 (2018).
58. Holland, H. D. *The Chemical Evolution of the Atmosphere and Oceans* (Princeton Univ. Press, 1984).
59. Fyfe, W. S. The water inventory of the Earth: fluids and tectonics. *Geol. Soc. Spec. Publ.* **78**, 1–7 (1994).
60. Arndt, N. T. & Nisbet, E. G. Processes on the young earth and the habitats of early life. *Annu. Rev. Earth Planet. Sci.* **40**, 521–549 (2012).
61. Russell, M. J. & Arndt, N. T. Geodynamic and metabolic cycles in the Hadean. *Biogeosciences* **2**, 97–111 (2005).
62. Lopresti, C., Lomas, H., Massignani, M., Smart, T. & Battaglia, G. Polymersomes: nature inspired nanometer sized compartments. *J. Mater. Chem.* **19**, 3576–3590 (2009).
63. Smart, T. et al. Block copolymer nanostructures. *Nanotoday* **3**, 38–46 (2008).
64. Bonaccio, S., Wessicken, M., Berti, D., Walde, P. & Luisi, P. L. Relation between the molecular structure of phosphatidyl nucleosides and the morphology of their supramolecular and mesoscopic aggregates. *Langmuir* **12**, 4976–4978 (1996).
65. Morse, J. W. & Mackenzie, F. T. Hadean ocean carbonate geochemistry. *Aquat. Geochem.* **4**, 301–319 (1998).
66. Holm, N. G. The significance of Mg in prebiotic geochemistry. *Geobiology* **10**, 269–279 (2012).

67. Ludwig, K. A., Kelley, D. S., Butterfield, D. A., Nelson, B. K. & Fru-Green, G. Formation and evolution of carbonate chimneys at the Lost City Hydrothermal Field. *Geochim. Cosmochim. Acta* **70**, 3625–3645 (2006).
68. Adamala, K. & Szostak, J. W. Nonenzymatic template-directed RNA synthesis inside model protocells. *Science* **342**, 1098–1101 (2013).
69. Jordan, S. F., Nee, E. & Lane, N. Isoprenoids enhance the stability of fatty acid membranes at the emergence of life potentially leading to an early lipid divide. *Interface Focus* **9**, 88–100 (2019).
70. Camprubi, E., Jordan, S. F., Vasiliadou, R. & Lane, N. Iron catalysis at the origin of life. *IUBMB Life* **69**, 373–381 (2017).
71. Lane, N., Allen, J. F. & Martin, W. How did LUCA make a living? Chemiosmosis in the origin of life. *BioEssays* **32**, 271–280 (2010).
72. Harrison, S. & Lane, N. Life as a guide to prebiotic nucleotide synthesis. *Nat. Commun.* **9**, 5176 (2018).

Acknowledgements

We thank M. Turmaine for assistance with NS-TEM, and B. Battaglia, F. Werner and D. Braben for discussions. We are grateful to the BBSRC (H.R., LIDo Doctoral Training Programme) and bgc3 for funding. A.M.H. and A.M. are funded by the Medical Research Council UK (Career Development Award grant no. MR/M00936X/1 to A.M.).

Author contributions

N.L. supervised the work. S.F.J., H.R., I.N.Z., A.M.H., A.M. and N.L. conceived and designed the experiments. S.F.J., H.R., I.N.Z. and A.M.H. performed the experiments. S.F.J., I.N.Z., A.M.H. and A.M. contributed materials and analysis tools. S.F.J. and N.L. analysed the data. S.F.J. and N.L. wrote the paper.

Competing interests

The authors declare no competing interests.

Additional information

Extended data is available for this paper at https://doi.org/10.1038/s41559-019-1015-y.

Supplementary information is available for this paper at https://doi.org/10.1038/s41559-019-1015-y.

Correspondence and requests for materials should be addressed to N.L.

Reprints and permissions information is available at www.nature.com/reprints.

Publisher's note Springer Nature remains neutral with regard to jurisdictional claims in published maps and institutional affiliations.

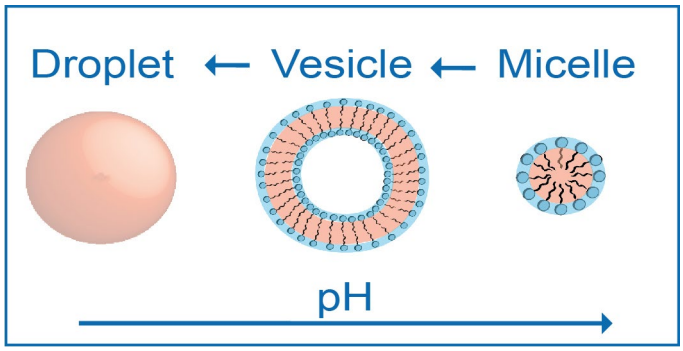

Extended Data Fig. 1 | Schematic representation of three different states of amphiphiles in aqueous solutions and their general relationship to pH. Blue shading highlights hydrophilic areas whereas pink shading represents hydrophobic areas. Fully deprotonated amphiphiles will form micelles with a hydrophobic interior and hydrophilic exterior. Mixtures of protonated and deprotonated amphiphiles can self-organise into bilayer membranes forming vesicles with an aqueous interior. Fully protonated amphiphiles form hydrophobic droplets in aqueous solutions.

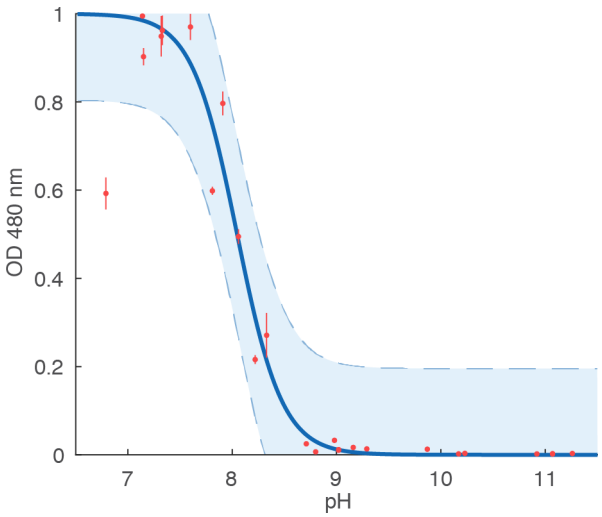

Extended Data Fig. 2 | Optical density plot for 10:1 fatty acid/1-alkanol mixture. Plot of normalised absorbance at 480 nm versus pH for 5 mM 10:1 C_{10}-C_{15} fatty acid/1-alkanol mixture.

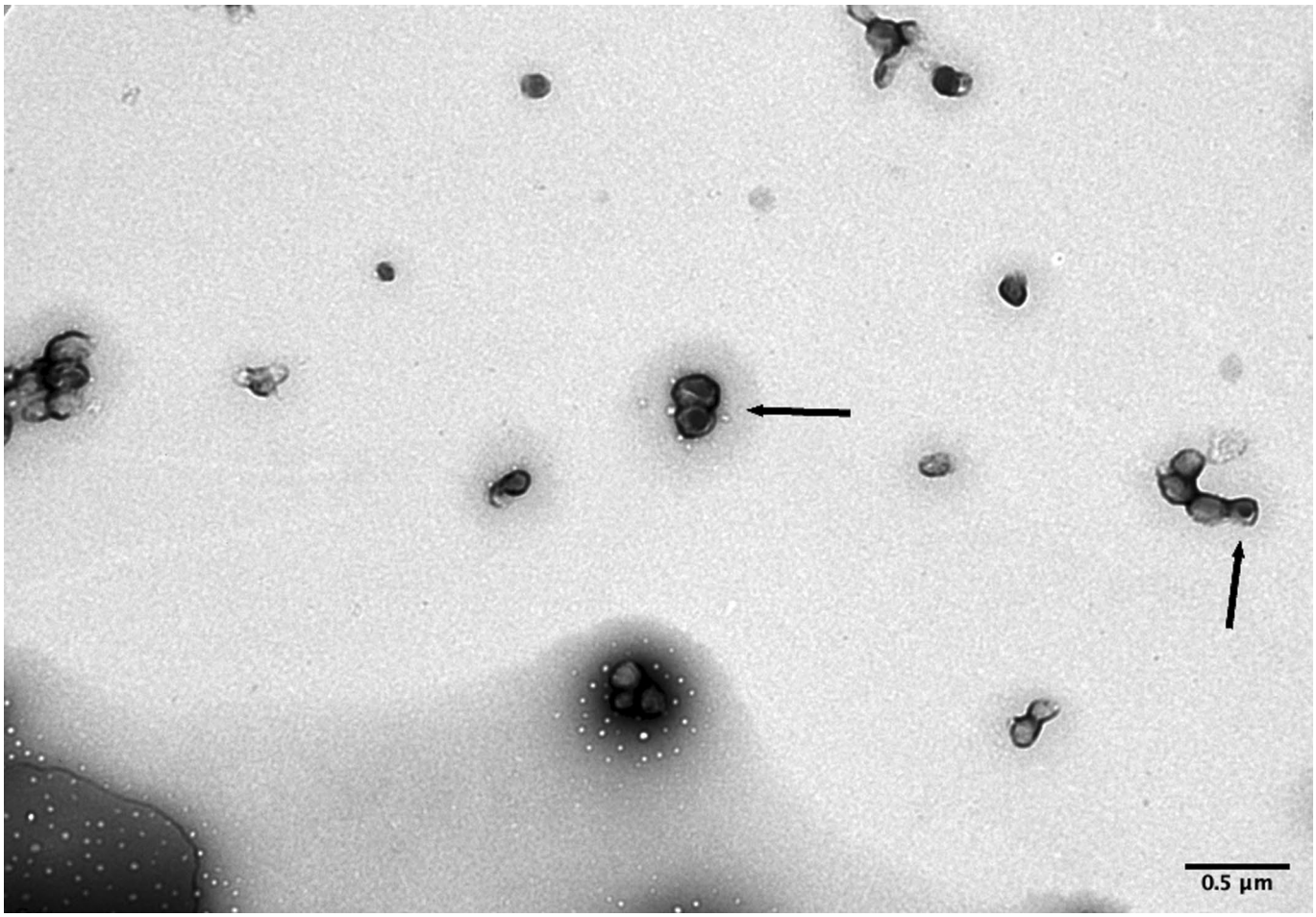

Extended Data Fig. 3 | NS-TEM micrograph of vesicles from 0.1 mM 1:1 C_{10}-C_{15} fatty acid/1-alkanol mixture. NS-TEM micrograph of 0.1 mM 1:1 C_{10}-C_{15} fatty acid/1-alkanol mixture vesicles at pH 7.17 (some examples of vesicles indicated by black arrows).

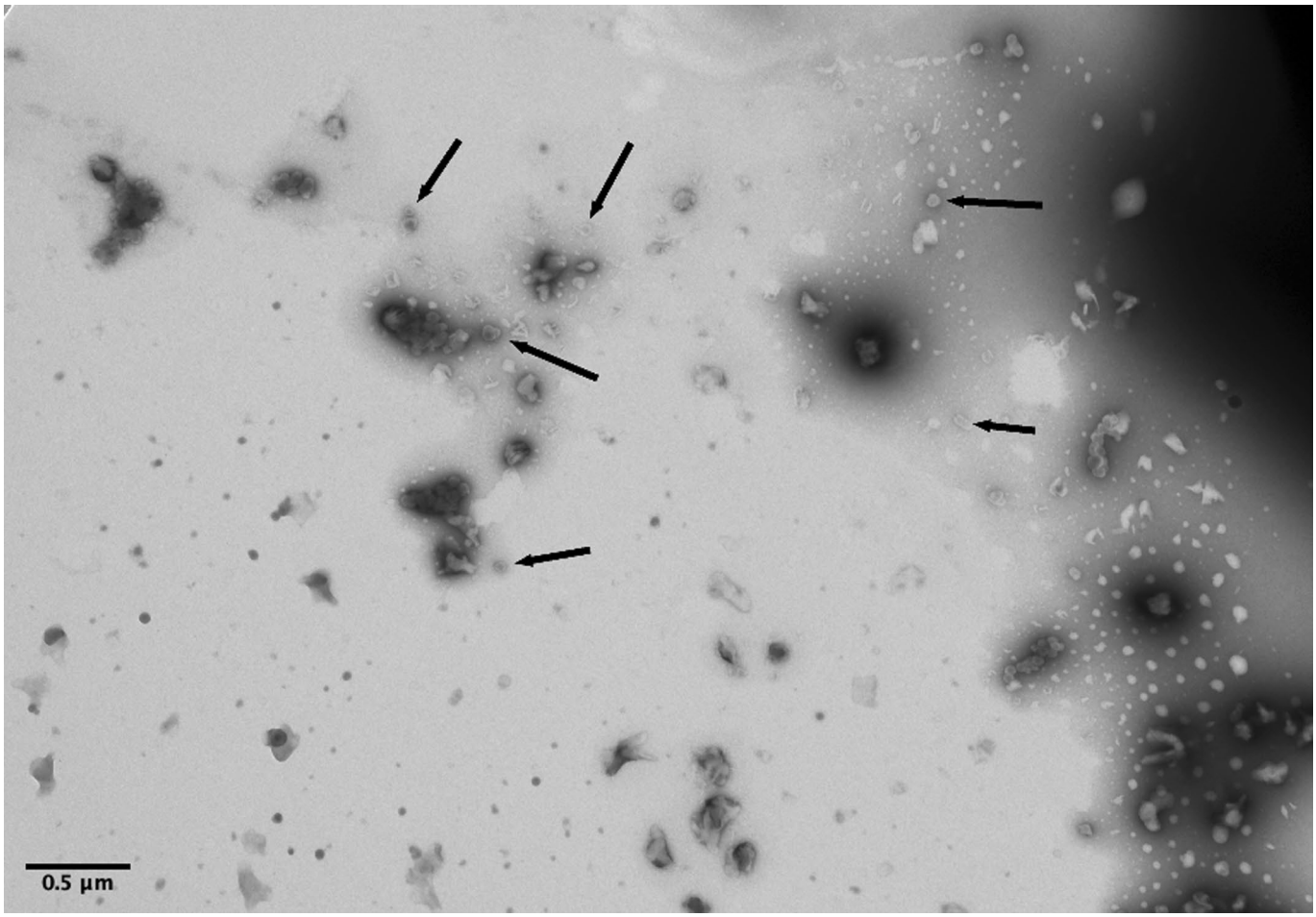

Extended Data Fig. 4 | NS-TEM micrograph of vesicles from 0.1 mM 1:1 C_{10}-C_{15} fatty acid/1-alkanol mixture. NS-TEM micrograph of 0.1 mM 1:1 C_{10}-C_{15} fatty acid/1-alkanol mixture vesicles at pH 8.29 (some examples of vesicles indicated by black arrows).

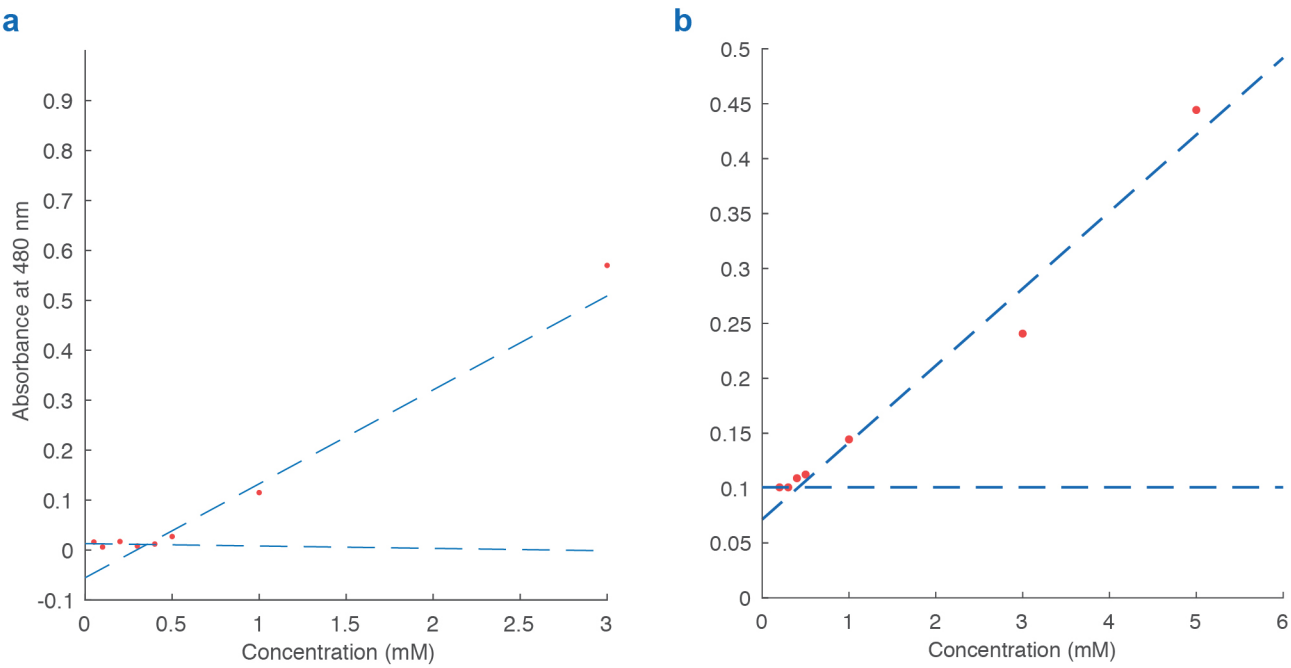

Extended Data Fig. 5 | Critical bilayer concentration (CBC) plots for 1:1 and 5:1 fatty acid/1-alkanol mixtures. Plot of absorbance at 480 nm versus concentration for 1:1 C_{10}-C_{15} fatty acid/1-alkanol mixture **(a)** and 5:1 C_{10}-C_{15} fatty acid/1-alkanol mixture **(b)**.

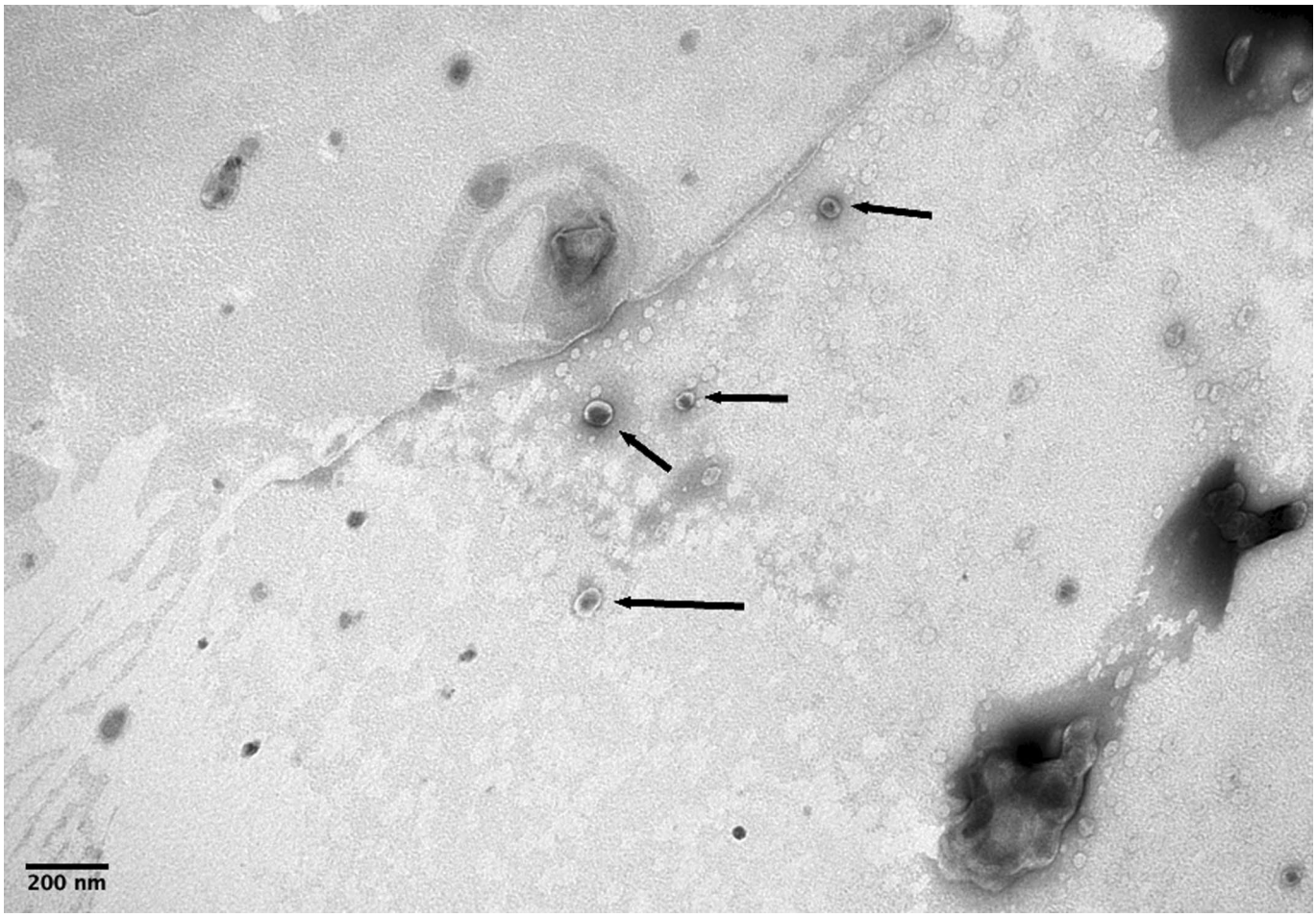

Extended Data Fig. 6 | NS-TEM micrograph of vesicles from 5 mM 1:1 C_{10}-C_{15} fatty acid/1-alkanol mixture in NaCl. NS-TEM micrograph of 5 mM 1:1 C_{10}-C_{15} fatty acid/1-alkanol mixture vesicles in 600 mM NaCl at pH 12.19 (some examples of vesicles indicated by black arrows).

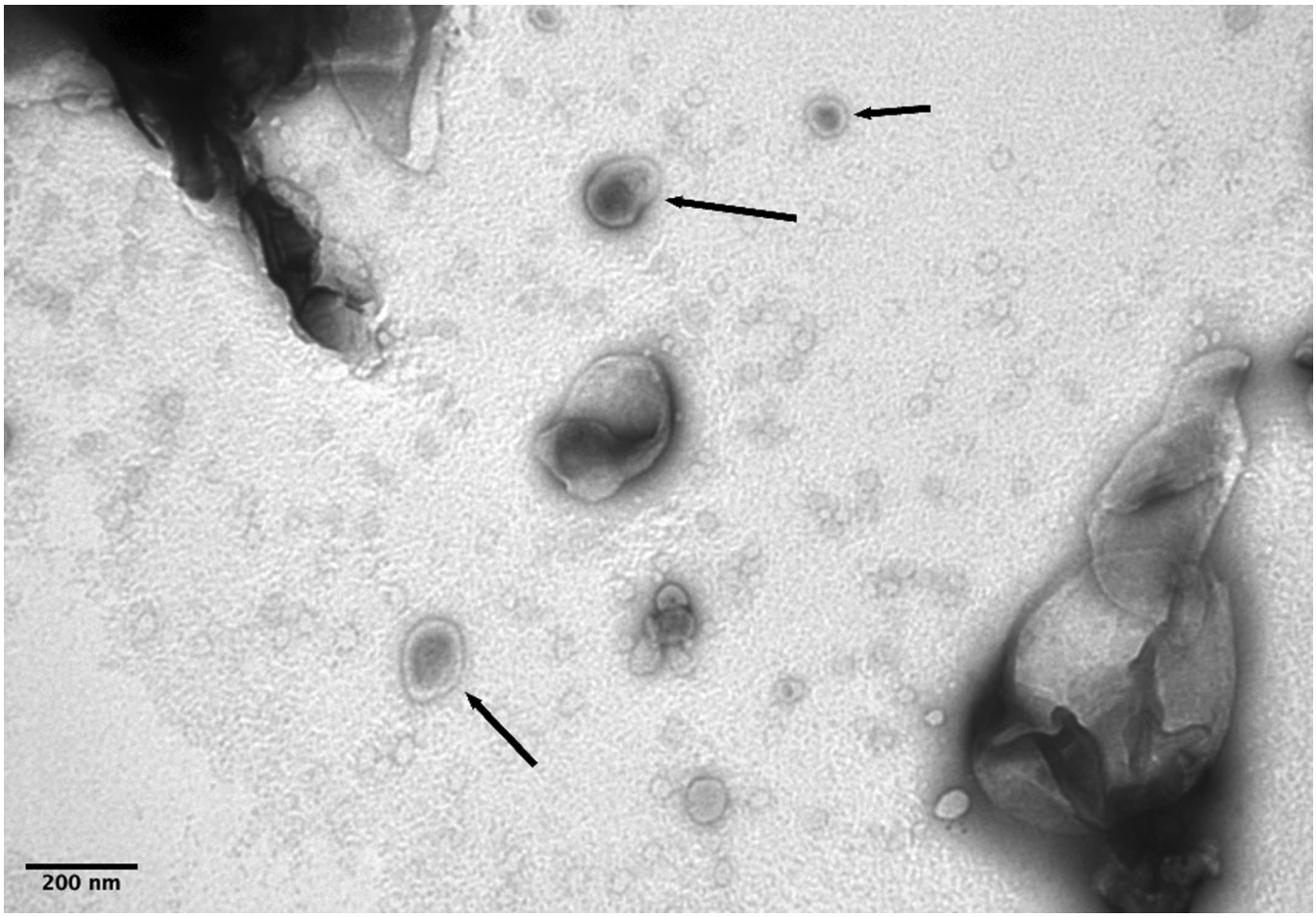

Extended Data Fig. 7 | NS-TEM micrograph of vesicles from 5 mM 1:1 C_{10}-C_{15} fatty acid/1-alkanol mixture in $MgCl_2$. NS-TEM micrograph of 5 mM 1:1 C_{10}-C_{15} fatty acid/1-alkanol mixture vesicles in 50 mM $MgCl_2$ at pH 11.83 (some examples of vesicles indicated by black arrows).

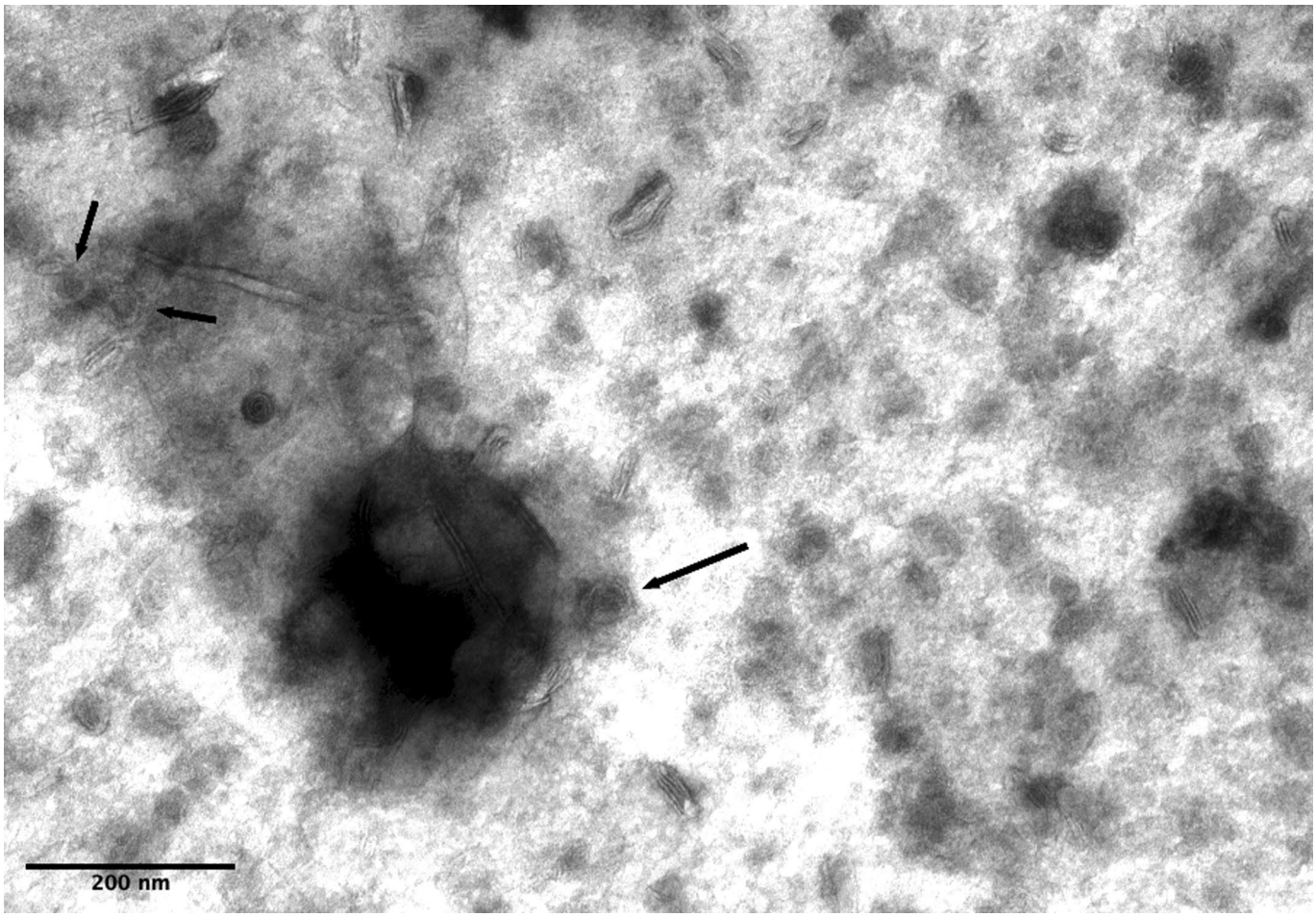

Extended Data Fig. 8 | NS-TEM micrograph of vesicles from 5 mM 1:1 C_{10}-C_{15} fatty acid/1-alkanol mixture in $CaCl_2$. NS-TEM micrograph of 5 mM 1:1 C_{10}-C_{15} fatty acid/1-alkanol mixture vesicles in 10 mM $CaCl_2$ at pH 12.18 (some examples of vesicles indicated by black arrows).

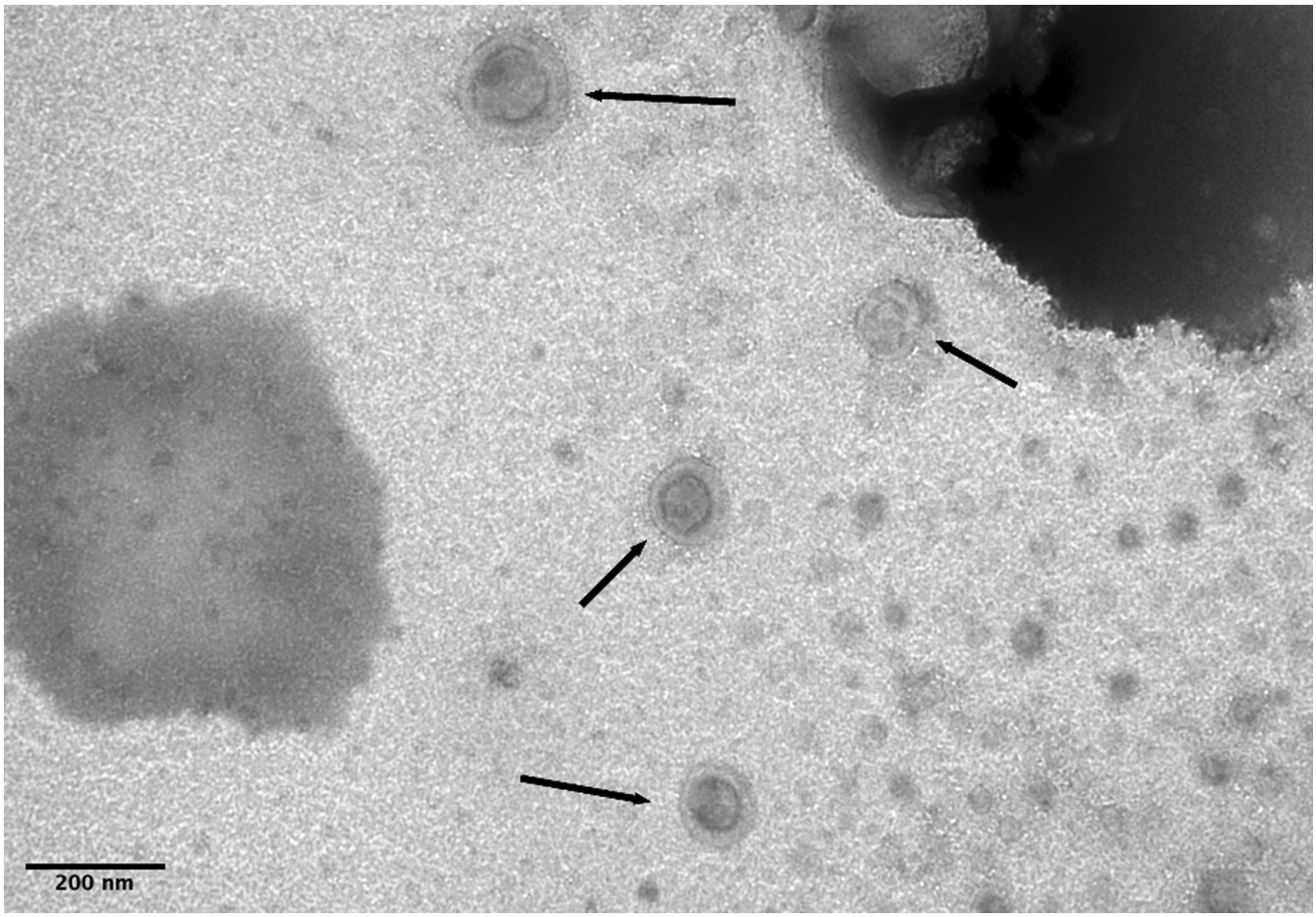

Extended Data Fig. 9 | NS-TEM micrograph of vesicles from 5 mM 1:1:1 C_{10}-C_{15} fatty acid/1-alkanol/C_{10} isoprenoid mixture vesicles in mixture of salts. NS-TEM micrograph of 5 mM 1:1:1 C_{10}-C_{15} fatty acid/1-alkanol/C_{10} isoprenoid mixture vesicles in mixture of salts (600 mM NaCl, 50 mM $MgCl_2$, 10 mM $CaCl_2$) at pH 11.73 (some examples of vesicles indicated by black arrows).

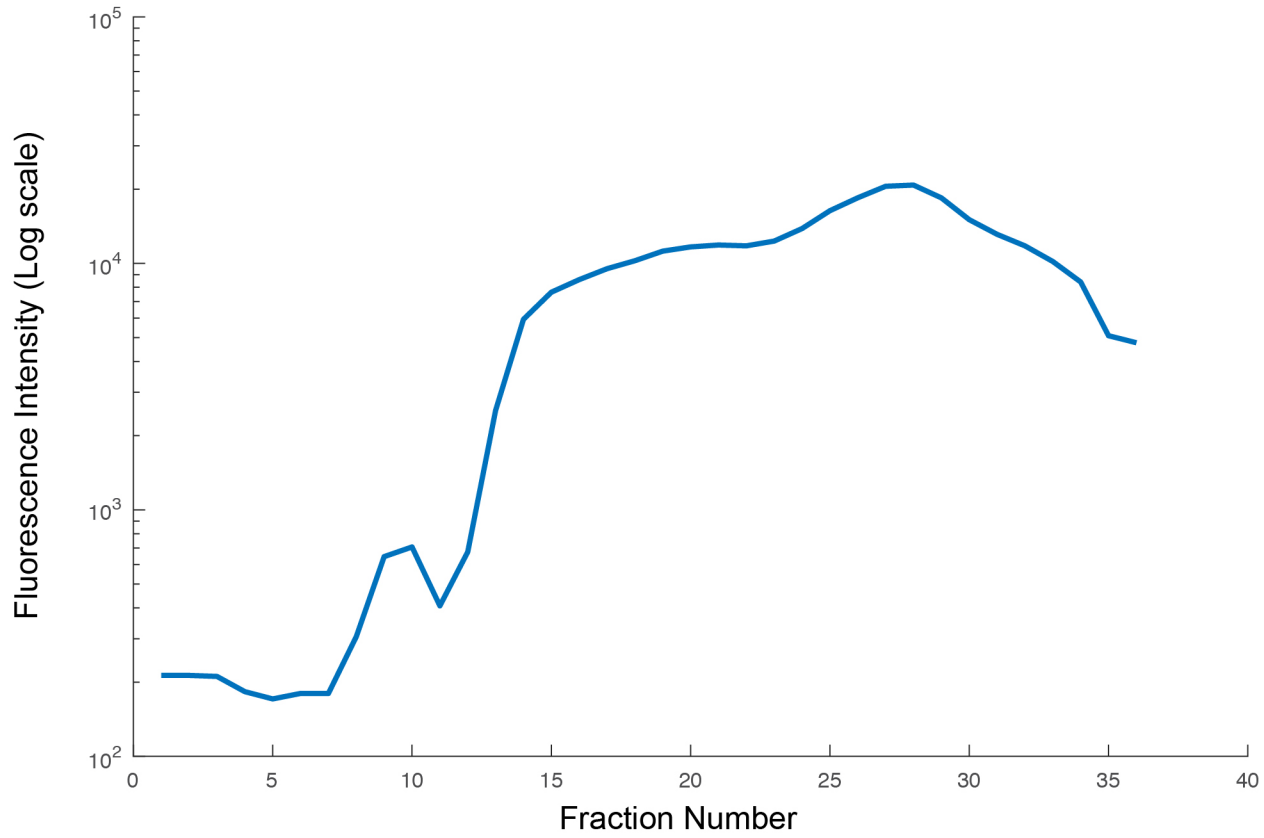

Extended Data Fig. 10 | Size exclusion chromatography (SEC) plot for 1:1:1 C_{10}-C_{15} fatty acid/1-alkanol/C_{10} isoprenoid mixture vesicles in mixture of salts. Plot of fluorescence intensity versus fraction number following size exclusion chromatography of 5 mM 1:1:1 C_{10}-C_{15} fatty acid/1-alkanol/C_{10} isoprenoid mixture vesicles in mixture of salts (600 mM NaCl, 50 mM $MgCl_2$, 10 mM $CaCl_2$) at pH 12 prepared in the presence of 5 mM calcein. The initial peak represents the vesicle fraction and is followed by the free calcein dye.

nature research

Corresponding author(s): Nick Lane

Last updated by author(s): Sep 13, 2019

Reporting Summary

Nature Research wishes to improve the reproducibility of the work that we publish. This form provides structure for consistency and transparency in reporting. For further information on Nature Research policies, see Authors & Referees and the Editorial Policy Checklist.

Statistics

For all statistical analyses, confirm that the following items are present in the figure legend, table legend, main text, or Methods section.

n/a	Confirmed
☒	☐ The exact sample size (*n*) for each experimental group/condition, given as a discrete number and unit of measurement
☒	☐ A statement on whether measurements were taken from distinct samples or whether the same sample was measured repeatedly
☒	☐ The statistical test(s) used AND whether they are one- or two-sided *Only common tests should be described solely by name; describe more complex techniques in the Methods section.*
☒	☐ A description of all covariates tested
☒	☐ A description of any assumptions or corrections, such as tests of normality and adjustment for multiple comparisons
☒	☐ A full description of the statistical parameters including central tendency (e.g. means) or other basic estimates (e.g. regression coefficient) AND variation (e.g. standard deviation) or associated estimates of uncertainty (e.g. confidence intervals)
☒	☐ For null hypothesis testing, the test statistic (e.g. *F*, *t*, *r*) with confidence intervals, effect sizes, degrees of freedom and *P* value noted *Give P values as exact values whenever suitable.*
☒	☐ For Bayesian analysis, information on the choice of priors and Markov chain Monte Carlo settings
☒	☐ For hierarchical and complex designs, identification of the appropriate level for tests and full reporting of outcomes
☒	☐ Estimates of effect sizes (e.g. Cohen's *d*, Pearson's *r*), indicating how they were calculated

Our web collection on statistics for biologists contains articles on many of the points above.

Software and code

Policy information about availability of computer code

Data collection	Zeiss Zen software (Zeiss, Germany) was used for confocal microscopy imaging. Gatan Microscopy Suite software (Gatan Inc., UK) was used for electron microscopy imaging.
Data analysis	FIJI image processing software (open source) was used for processing of microscopy data. Matlab software (Mathworks Inc., US) was used for processing optical density data.

For manuscripts utilizing custom algorithms or software that are central to the research but not yet described in published literature, software must be made available to editors/reviewers. We strongly encourage code deposition in a community repository (e.g. GitHub). See the Nature Research guidelines for submitting code & software for further information.

Data

Policy information about availability of data

All manuscripts must include a data availability statement. This statement should provide the following information, where applicable:

- Accession codes, unique identifiers, or web links for publicly available datasets
- A list of figures that have associated raw data
- A description of any restrictions on data availability

Provide your data availability statement here.

Field-specific reporting

Please select the one below that is the best fit for your research. If you are not sure, read the appropriate sections before making your selection.

☒ Life sciences ☐ Behavioural & social sciences ☐ Ecological, evolutionary & environmental sciences

Life sciences study design

All studies must disclose on these points even when the disclosure is negative.

Sample size	Sample size was determined based on the number of variables to be tested. Variables were selected based on previously published research assessing stability of vesicles under prebiotic conditions.
Data exclusions	No data were excluded from the analysis.
Replication	All analyses were performed in triplicate. Reported error bars represent the standard deviation. All replicates were successful and all experiments were reproducible.
Randomization	Not applicable
Blinding	Not applicable

Reporting for specific materials, systems and methods

We require information from authors about some types of materials, experimental systems and methods used in many studies. Here, indicate whether each material, system or method listed is relevant to your study. If you are not sure if a list item applies to your research, read the appropriate section before selecting a response.

Materials & experimental systems

n/a	Involved in the study
☒	☐ Antibodies
☒	☐ Eukaryotic cell lines
☒	☐ Palaeontology
☒	☐ Animals and other organisms
☒	☐ Human research participants
☒	☐ Clinical data

Methods

n/a	Involved in the study
☒	☐ ChIP-seq
☒	☐ Flow cytometry
☒	☐ MRI-based neuroimaging